

Explanation-Preserving Augmentation for Semi-Supervised Graph Representation Learning

Zhuomin Chen
zchen051@fiu.edu

Knight Foundation School of
Computing and Information Sciences,
Florida International University
Miami, USA

Jingchao Ni
jni7@uh.edu

Department of Computer Science,
University of Houston
Houston, USA

Hojat Allah Salehi
hsalehi@fiu.edu

Knight Foundation School of
Computing and Information Sciences,
Florida International University
Miami, USA

Xu Zheng
xzhen019@fiu.edu

Knight Foundation School of
Computing and Information Sciences,
Florida International University
Miami, USA

Esteban Schafir
escha032@fiu.edu

Knight Foundation School of
Computing and Information Sciences,
Florida International University
Miami, USA

Farhad Shirani
fshirani@fiu.edu

Knight Foundation School of
Computing and Information Sciences,
Florida International University
Miami, USA

Dongsheng Luo
dluo@fiu.edu

Knight Foundation School of
Computing and Information Sciences,
Florida International University
Miami, USA

Abstract

Graph representation learning (GRL), enhanced by graph augmentation methods, has emerged as an effective technique achieving performance improvements in wide tasks such as node classification and graph classification. In self-supervised GRL, paired graph augmentations are generated from each graph. Its objective is to infer similar representations for augmentations of the same graph, but maximally distinguishable representations for augmentations of different graphs. Analogous to image and language domains, the desiderata of an ideal augmentation method include both (1) semantics-preservation; and (2) data-perturbation; *i.e.*, an augmented graph should preserve the semantics of its original graph while carrying sufficient variance. However, most existing (un-)/self-supervised GRL methods focus on data perturbation but largely neglect semantics preservation. To address this challenge, in this paper, we propose a novel method, Explanation-Preserving Augmentation (EPA), that leverages graph explanation techniques for generating augmented graphs that can bridge the gap between semantics-preservation and data-perturbation. EPA first uses a small number of labels to train a graph explainer for inferring the sub-structures (explanations) that are most relevant

to a graph’s semantics. These explanations are then used for generating semantics-preserving augmentations for self-supervised GRL, namely EPA-GRL. We demonstrate theoretically, using an analytical example, and through extensive experiments on a variety of benchmark datasets that EPA-GRL outperforms the state-of-the-art (SOTA) GRL methods, which are built upon semantics-agnostic data augmentations.

Keywords

Graph Neural Networks, Explainable AI, Data Augmentation

ACM Reference Format:

Zhuomin Chen, Jingchao Ni, Hojat Allah Salehi, Xu Zheng, Esteban Schafir, Farhad Shirani, and Dongsheng Luo. 2018. Explanation-Preserving Augmentation for Semi-Supervised Graph Representation Learning. In *Proceedings of Make sure to enter the correct conference title from your rights confirmation email (Conference acronym ’XX)*. ACM, New York, NY, USA, 16 pages. <https://doi.org/XXXXXXXX.XXXXXXX>

1 Introduction

Inspired by recent progress in unsupervised and self-supervised representation learning in visual and language domains [6], graph representation learning (GRL) has led to significant performance improvements in tasks such as node classification [35, 36] and graph classification [31, 43] across a wide spectrum of domains ranging from social science [36] to molecular biology [31]. In particular, contrastive learning has emerged as a dominant technique for GRL, in which two augmentations are generated for each graph with the objective of generating similar representations for augmentations of the same graph but maximally discriminative representations for augmentations of different graphs. A determining factor in

Permission to make digital or hard copies of all or part of this work for personal or classroom use is granted without fee provided that copies are not made or distributed for profit or commercial advantage and that copies bear this notice and the full citation on the first page. Copyrights for components of this work owned by others than the author(s) must be honored. Abstracting with credit is permitted. To copy otherwise, or republish, to post on servers or to redistribute to lists, requires prior specific permission and/or a fee. Request permissions from permissions@acm.org.
Conference acronym ’XX, June 03–05, 2018, Woodstock, NY

© 2018 Copyright held by the owner/author(s). Publication rights licensed to ACM.
ACM ISBN 978-1-4503-XXXX-X/18/06
<https://doi.org/XXXXXXXX.XXXXXXX>

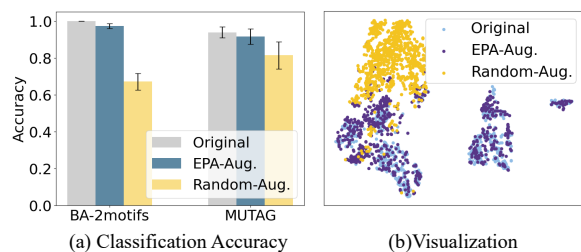


Figure 1: Accuracy of different augmentation methods in a graph classification task.

the performance of GRL methods is the use of an effective graph augmentation strategy. Analogous to image data augmentation [6, 12], an ideal pair of graph augmentations should concurrently be able to (1) inherit the semantics of their original graph; and (2) present sufficient variance from each other [28, 29, 38, 40, 44].

However, most of the existing works [28, 40, 44] only focus on structural perturbations that can introduce variance to the augmented graphs but largely neglect the need for preserving semantics. For example, in graph contrastive learning (GraphCL) [43] and JOAO [42], an augmented graph is typically generated by perturbing its original graph through random edge dropping, node dropping, feature masking, and subgraph extraction. The inherent randomness in these perturbations inevitably induces substantial alterations of some important (sub-)graph structures or features that could result in considerable loss of semantics, which in turn, may lead to significant performance drops in downstream tasks.

Fig. 1 illustrates a specific experiment that evaluates the semantics-preserving capability of different augmentation techniques, where a Graph Neural Network (GNN) classifier [16] is first trained on the training partition of a benchmark dataset (*i.e.*, BA-2motifs [18] and MUTAG [8]), and its accuracy is then evaluated on the original graphs in the test set and on the augmented graphs derived from them. Two augmentation methods are included. “Random-Aug” represents randomly dropping nodes from the original graph in a semantics-agnostic manner. “EPA-Aug” is a semantics-preserving augmentation (which will be introduced later). From Fig. 1(a), the fully trained GNN can accurately classify the graphs in the original test set. However, it has a sharp drop in accuracy on the “Random-Aug” graphs, suggesting a significant loss of semantics (*i.e.*, class signals). The accuracy on “EPA-Aug” graphs is close to that of the original graphs, implying effective semantics-preservation. Fig. 1(b) shows the distribution of the graph embeddings in BA-2motifs. A large distribution shift from the original graphs to the “Random-Aug” graphs can be observed. Furthermore, it can be observed that “EPA-Aug” well preserves the distribution of the original embeddings while demonstrate sufficient variance. This example implies that semantics-preserving augmentations has the potential to yield substantial performance improvements in GRL.

To avoid the loss of semantic information due to the graph augmentations adopted by GraphCL [43] and JOAO [42], the MoCL [27] method substitutes valid substructures in molecular graphs with bioisosteres that share similar properties. However, this requires expensive domain knowledge and does not naturally extend to other domains such as social graphs. More recently, SimGRACE

[34] addresses this challenge by circumventing graph perturbations. Instead, it perturbs GNN parameters and uses the perturbed GNN to generate augmented graphs. Although it does not explicitly alter graph structures, it may implicitly do so by arbitrarily changing graph embeddings that may be reflected to unconstrained structural changes. Thus it cannot guarantee semantics-preservation.

In image data augmentation, semantics can be visually observed, thus enabling human prior in the determination of perturbation techniques (*e.g.*, rotation, cropping, Gaussian noise, *etc.*). However, semantics in graphs are not as easily visible and are typically class-specific. Our objective is to develop semantics-preserving augmentation techniques — using models trained by leveraging only a few labeled input samples — to enable improved GRL. A related line of work is supervised graph contrastive learning [13, 14]. However, they often require a large amount of labeled input samples for determining positive pairs instead of using the class signals for explicit semantics preservation.

Inspired by recent research on explainable AI (XAI) for graphs [18, 41, 47], we propose a novel approach, Explanation-Preserving Augmentation enhanced GRL (EPA-GRL), which leverages graph explanation techniques for generating augmented graphs that can bridge the gap between semantics-preservation and data-perturbation. Methods for explaining GNNs usually learn a parametric graph explainer that can identify a sub-structure (*e.g.*, benzene ring) in the original graph (*e.g.*, molecule) that distinguishes the graph from the graphs of other classes [18]. In other words, the explainer infers semantics represented by sub-graph patterns. In light of this, EPA-GRL is designed as a two-stage approach. At the pre-training stage, it learns a graph explainer using a handful of class labels. At the GRL stage, for each input graph, EPA-GRL uses the explainer to extract a semantics subgraph and perturbs the rest of the original graphs (*i.e.*, marginal subgraph). The semantics subgraph and the perturbed marginal subgraph are combined to form an augmented graph, which is fed to a contrastive learning framework for representation learning. In this way, EPA-GRL uses a few labeled graphs and relatively more unlabeled graphs, establishing a novel semi-supervised GRL framework using limited labels. In summary, the main contributions are as follows.

- We identify a major limitation of the existing augmentation methods in GRL by reviewing the two criteria of data augmentation.
- This work is the first to explore the potential of a few class labels in semantics-preservation for GRL.
- We propose a new semi-supervised GRL framework with a novel augmentation method EPA, which introduces XAI to GRL for semantics-preserving perturbation.
- We show theoretically, through an analytical example, that the accuracy gap of an empirical risk minimizer operating on the output embeddings of a GRL model under semantics-preserving and semantics-agnostic augmentations can be arbitrarily large.
- We conduct extensive experiments on 6 benchmark datasets with comparison of many augmentation methods and contrastive learning frameworks. The results validate the effectiveness of the proposed EPA-GRL, especially when labeled data are limited.

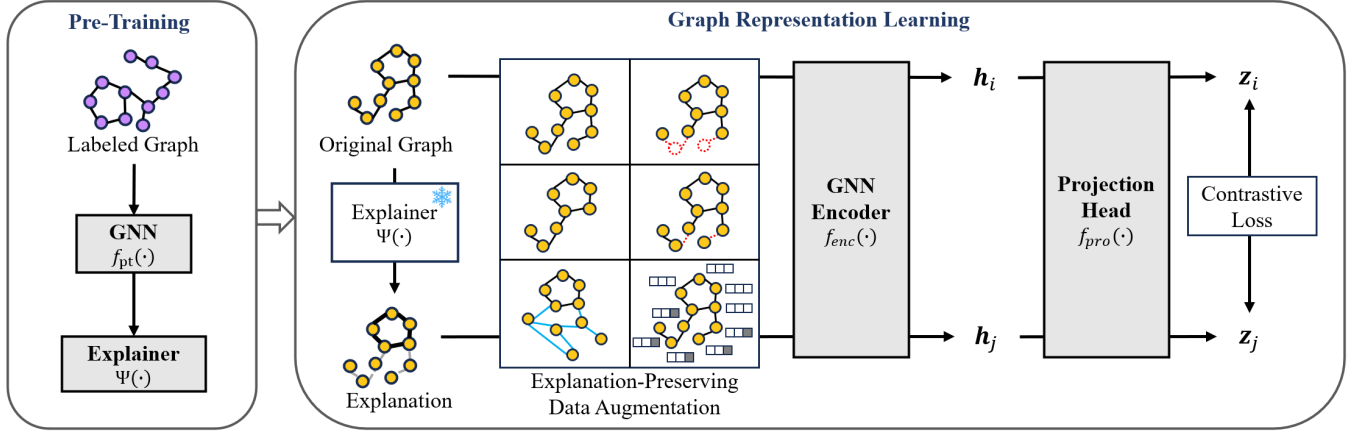


Figure 2: The proposed EPA-GRL Architecture. We first pretrain a GNN model $f_{pt}(\cdot)$ and its explainer $\Psi(\cdot)$ with a small number of labeled training samples. Then in the representation learning step, we use the frozen explainer $\Psi(\cdot)$ to produce augmented graphs to train a GNN encoder $f_{enc}(\cdot)$ and a projection head $f_{pro}(\cdot)$ with a contrastive loss. The output of the GNN encoder $f_{enc}(\cdot)$ will be used as graph representations.

2 Notations and Problem Formulation

A graph G is defined by the following components: i) a node set $\mathcal{V} = \{v_1, v_2, \dots, v_n\}$, where n is the number of nodes; ii) an edge set $\mathcal{E} \subseteq \mathcal{V} \times \mathcal{V}$; iii) a feature matrix $X \in \mathbb{R}^{n \times d}$, where the i -th row X_i is node v_i 's d -dimensional feature; and iv) an adjacency matrix $A \in \{0, 1\}^{n \times n}$, where $A_{i,j} = 1$ if $(v_i, v_j) \in \mathcal{E}$. Additionally, each graph is associated with a label $Y \in \mathcal{Y}$, where \mathcal{Y} is a finite set.

Formally, we assume a pair of training sets, a (small) labeled set $\mathcal{T}_\ell = \{(G_i, Y_i) | i \in [M]\}$, and a (large) unlabeled set $\mathcal{T}_u = \{G_i | i \in [N]\}$, where $M \ll N$. Our objective is to leverage the small number of labeled graphs in \mathcal{T}_ℓ and relatively more unlabeled graphs in \mathcal{T}_u to perform semantics-preserving representation learning. Similar to the supervised contrastive learning methods [13, 14], labels from a classification task are leveraged for model training. However, *our problem is substantially different from the existing works by only using a few labels, leading to a constrained semi-supervised GRL problem.*

3 The Proposed Method

In this section, we introduce the proposed EPA-GRL method. An overview is shown in Fig. 2. The proposed GRL framework first pre-train a GNN explainer using the labeled graphs in \mathcal{T}_ℓ , where the explainer $\Psi(\cdot) : G \mapsto G^{(exp)}$ takes a graph G as input and outputs an explanation subgraph $G^{(exp)}$ that is class-relevant. Next, a semantic-preserving stochastic mapping $P_{G'|G}$ transforms the original graph G to an augmentation G' such that $G^{(exp)} \subseteq G'$, where the mapping can perform random perturbations on the non-explanation (marginal) part of the input G , *i.e.*, $G \setminus G^{(exp)}$; Finally, the augmented graph G' is fed to an encoder $f_{enc} : G' \mapsto \mathbf{h}$, where $\mathbf{h} \in \mathbb{R}^{d_e}$ is the d_e -dimensional embedding of G' . f_{enc} is trained using contrastive learning on both augmentations of the unlabeled training set \mathcal{T}_u and the labeled training set \mathcal{T}_ℓ .

3.1 Pre-Training GNN Explainer

In this step, the goal is to train a GNN explainer to identify the most responsible subgraph for its predictions. Extracting such key substructures enables preservation of core semantics of the input graph when perturbing the rest of the graph. We begin by training a GNN $f_{pt}(\cdot)$ using the labeled training set. The GNN learns to capture both structural and feature-based information necessary to distinguish different graph classes. The GNN is trained by minimizing the cross-entropy loss between the predicted label $f_{pt}(G)$ and the ground-truth label y . Formally, the optimization problem is:

$$\arg \min_{f_{pt}} \left(\sum_{(G,y) \in \mathcal{T}_\ell} -y \log(f_{pt}(G)) \right). \quad (1)$$

Next, we propose to use a GNN explainer to extract subgraphs that retain the semantics necessary for classification. Augmentations can then be achieved by making controlled perturbations to rest, marginal parts of the graph. Formally, given a graph $G = (A, X)$, the explainer generates an explanation subgraph $G^{(exp)} = (X, A \odot M)$, where $M \in \{0, 1\}^{|\mathcal{V}| \times |\mathcal{V}|}$ is a binary mask and each entry $M_{ij} = 1$ indicates edge (i, j) is retained in the subgraph $G^{(exp)}$. To improve efficiency, we use a generative explainer, $\Psi(\cdot)$, which employs a parametric neural network to learn the mask M based on node embeddings [18, 19]. The explainer $\Psi(\cdot)$ is trained on the labeled dataset \mathcal{T}_ℓ and can be directly applied to the unlabeled graphs in \mathcal{T}_u to generate new explanation subgraphs.

The objective of the GNN explainer $\Psi(\cdot)$ is to find a subgraph, denoted by $\Psi(G)$, that balances semantic preservation and compactness. This is achieved by following the Graph Information Bottleneck (GIB) principle, which has been widely used in GNN explanation methods [28, 38, 40, 44, 45]. The GIB principle states that an optimal subgraph should retain sufficient information for a prediction task while being as compact as possible, to avoid overfitting or including irrelevant parts of the graph. The learning objective

for the explainer is defined as:

$$\arg \min_{\Psi} \left(\sum_{(G,y) \in \mathcal{T}_\ell} \text{CE}(Y; f_{\text{pt}}(\Psi(G))) + \lambda |\Psi(G)| \right), \quad (2)$$

where $\text{CE}(Y; f_{\text{pt}}(\Psi(G)))$ is the cross-entropy loss between the label and the prediction on the subgraph $\Psi(G)$, and $|\Psi(G)|$ is the size of the subgraph, which can be measured by the number of edges or the sum of edge weights. The hyper-parameter λ controls the trade-off between the terms for information preservation and structural compactness.

3.2 Explanation-Preserving Augmentation Enhanced Graph Representation Learning

Data augmentation plays a critical role in contrastive learning, which generates multiple augmented views of the same graph for learning invariant representations. The success of graph data augmentation attributes to its ability to preserve the core semantics of the graph while introducing variances that facilitates robust representation learning. However, a major limitation of the existing methods is their unconstrained perturbation techniques that may arbitrarily modify the graph structure or node features, and inadvertently disconnect important substructures, leading to a significant loss of semantic information.

Explanation-Preserving Augmentation. To address this limitation, we propose an explanation-preserving augmentation (EPA) strategy that explicitly retains the essential part of the graph regarding its class. Specifically, we use the pre-trained graph explainer $\Psi(\cdot)$ to extract an explanation subgraph $G^{(\text{exp})} = \Psi(G)$, which contains the most relevant substructures to the graph’s semantics and $G^{(\text{exp})}$ will be kept intact. The remaining part of the graph, denoted as the *marginal subgraph* $\Delta G = G \setminus G^{(\text{exp})}$, is perturbed to introduce necessary variance for contrastive learning. Next, we introduce EPA-based methods for graph-structured data and discuss their intuitive priors. A summary of data augmentation methods is shown in Table 1. Detailed algorithms are provided in Appendix B.

- **Node Dropping** randomly removes a subset of nodes and their edges from the marginal subgraph ΔG . The assumption is that removing irrelevant nodes has a small impact on the core semantics of the graph. Each node’s dropping probability follows an i.i.d. uniform distribution.
- **Edge Dropping** modifies the connectivity in G by randomly dropping edges in the marginal subgraph ΔG . It assumes the semantic meaning of the graph is robust to the changes of inessential edges. Each dropping follows an i.i.d. uniform distribution.
- **Attribute Masking** hides a subset of node or edge attributes in the marginal subgraph ΔG . The assumption is related to node dropping – missing unimportant node attributes has minor impacts on the recovery of essential semantics by the explanation subgraph.
- **Subgraph** is a method that samples a subgraph from the marginal subgraph ΔG using random walk. The assumption is that sampling a connected subgraph in ΔG vary the graph structure but does not disrupt the overall semantic integrity.
- **Mixup** randomly selects a different graph G from the batch of graph G , and combines its marginal subgraph $\Delta \tilde{G}$ with the explanation subgraph $G^{(\text{exp})}$ of the original graph G .

Graph Representation Learning. After generating the explanation-preserving augmentations, we employ a contrastive learning framework to learn graph representations. Our EPA approach is versatile and can be integrated into various graph contrastive learning methods. Here, we demonstrate its application with two popular techniques: GraphCL [43] and SimSiam [7].

For each graph G in the dataset, two augmented views G_1 and G_2 are generated using our EPA techniques. These augmented graphs are then passed to a graph encoder $f_{\text{enc}}(\cdot)$, which can be any suitable GNN architecture. The encoder produces graph-level representations $\mathbf{h}_1 = f_{\text{enc}}(G_1)$ and $\mathbf{h}_2 = f_{\text{enc}}(G_2)$ for the two augmented views. Following the approach in [6], a projection head, implemented as an MLP, is adopted to obtain new representations for defining the self-supervised learning loss. Specifically, we compute $\mathbf{z}_1 = f_{\text{pro}}(\mathbf{h}_1)$ and $\mathbf{z}_2 = f_{\text{pro}}(\mathbf{h}_2)$. In line with the previous works [6, 7], \mathbf{z}_1 and \mathbf{z}_2 are used exclusively for model training. For downstream tasks, we discard the projection head and utilize \mathbf{h}_1 and \mathbf{h}_2 as the graph representations.

GraphCL [43] is a contrastive learning framework developed for graphs with the aim of maximizing the mutual information between different augmented views of the same graph. It uses a noise-contrastive estimation approach to differentiate between positive and negative samples. Given a batch of N graphs, we re-annotate $\mathbf{z}_1, \mathbf{z}_2$ as $\mathbf{z}_{i,1}, \mathbf{z}_{i,2}$ for the i -th graph in the minibatch. Then the contrastive loss [50] is:

$$\begin{aligned} \ell_i^{(\text{graphcl})} = & -\frac{1}{2} \log \frac{\exp(\text{sim}(\mathbf{z}_{i,1}, \mathbf{z}_{i,2})/\tau)}{\sum_{j=1}^N \exp(\text{sim}(\mathbf{z}_{i,1}, \mathbf{z}_{j,2})/\tau)} \\ & -\frac{1}{2} \log \frac{\exp(\text{sim}(\mathbf{z}_{i,2}, \mathbf{z}_{i,1})/\tau)}{\sum_{j=1}^N \exp(\text{sim}(\mathbf{z}_{i,2}, \mathbf{z}_{j,1})/\tau)}, \end{aligned} \quad (3)$$

where τ denotes the temperature parameter, $\text{sim}(\cdot, \cdot)$ is the cosine similarity function. The final loss is computed across all positive pairs in the batch.

SimSiam [7] is a straightforward siamese network approach that learns representations by maximizing the similarity between differently augmented views of the same sample. Unlike GraphCL, it doesn’t rely on negative samples. The SimSiam architecture processes two augmented views of a graph through the same encoder network. After encoding, SimSiam applies an MLP predictor to one view and a stop-gradient operation to the other view. The model then maximizes the similarity between these two processed views. Specifically, for two augmented views of a graph, we have:

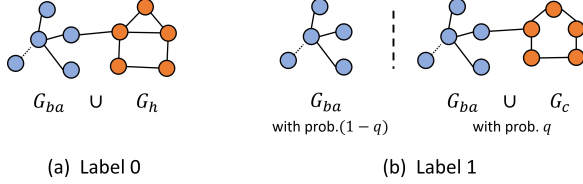
$$\mathbf{p}_1 = \text{MLP}(\mathbf{z}_1) \quad \mathbf{p}_2 = \text{MLP}(\mathbf{z}_2), \quad (4)$$

where \mathbf{z}_1 and \mathbf{z}_2 are the encoded graph representations of the two views. \mathbf{p}_1 and \mathbf{p}_2 are their respective predictions after passing through the MLP. The objective is to minimize their negative cosine similarity:

$$\begin{aligned} \mathcal{D}(\mathbf{p}_1, \text{stopgrad}(\mathbf{z}_2)) &= -\frac{\mathbf{p}_1}{\|\mathbf{p}_1\|_2} \cdot \frac{\text{stopgrad}(\mathbf{z}_2)}{\|\text{stopgrad}(\mathbf{z}_2)\|_2} \\ \mathcal{D}(\mathbf{p}_2, \text{stopgrad}(\mathbf{z}_1)) &= -\frac{\mathbf{p}_2}{\|\mathbf{p}_2\|_2} \cdot \frac{\text{stopgrad}(\mathbf{z}_1)}{\|\text{stopgrad}(\mathbf{z}_1)\|_2}. \end{aligned} \quad (5)$$

Table 1: Overview of explanation-preserving data augmentations for graphs.

Data Augmentation	Type	Underlying Prior
Node Dropping	Nodes, edges	Missing inessential nodes does not affect semantics.
Edge Dropping	Edges	The graph is robust to non-critical edge connectivity changes.
Attribute Masking	Nodes	Loss of inessential attributes does not alter semantics.
Subgraph	Nodes, edges	Local inessential sub-structures does not disrupt core semantics.
Mixup	Nodes, edges	Mixing a semantic subgraph with another marginal subgraph preserves semantics.

**Figure 3: Exemplar graphs in modified BA-2motifs.**

The stop-gradient (stopgrad) operation is a key component of SimSiam. It blocks the gradients of $\text{stopgrad}(z_1)$ and $\text{stopgrad}(z_2)$ during backpropagation, treating these terms as constants when computing gradients. This process prevents direct optimization of the encoder through these paths, which is crucial for avoiding trivial solutions and encouraging the model to learn meaningful representations. The objective function is implemented as follows:

$$\ell^{(\text{simsiam})} = \frac{1}{2} \mathcal{D}(\mathbf{p}_1, \text{stopgrad}(z_2)) + \frac{1}{2} \mathcal{D}(\mathbf{p}_2, \text{stopgrad}(z_1)). \quad (6)$$

4 Theoretical Analysis

To investigate the importance of preserving semantics in augmented graphs for GRL, in this section, we theoretically analyze the errors of classifying graph embeddings produced by (1) an encoder trained with semantics-preserving augmentations, denoted by $f_{\text{enc}}^{\text{SP}}(\cdot)$; and (2) an encoder trained with semantics-agnostic augmentations, denoted by $f_{\text{enc}}^{\text{SA}}(\cdot)$. Our main theorem (Theorem 1) shows that in certain classification scenarios, the error under $f_{\text{enc}}^{\text{SP}}(\cdot)$ is close to zero, whereas for $f_{\text{enc}}^{\text{SA}}(\cdot)$ it is close to $\frac{1}{2}$, which is equivalent to random guessing.

To demonstrate our analysis, we modify the widely studied benchmark BA2-Motifs [18]. As shown in Fig. 3, the dataset has two classes of graphs. The first class consists of graphs generated by taking the union of a Barabási-Albert (BA) graph [2] and a house motif. The second class also has a BA graph as the base, which is optionally attached to a cycle motif with probability $q \in (0, 1)$. Formally, let $P_{G_{ba}}$ be a probability distribution of BA graphs, let G_h represent the house motif subgraph, with five nodes and six edges, and let G_c represent the cycle motif with five nodes and five edges. Graphs with label 0 are of the form $G_{ba} \cup G_h$, i.e., attach G_h to G_{ba} , where $G_{ba} \sim P_{G_{ba}}$. Graphs with label 1 can either be G_{ba} or $G_{ba} \cup G_c$, with probabilities $1 - q$ and q , respectively.

We consider two types of edge-dropping-based augmentations as follows.

- **Semantics-Agnostic Augmentation** ($P_{G'|G}^{\text{SA}}$). Each edge in a graph is dropped independently with a probability $p \in (0, 1)$.
- **Semantics-Preserving Augmentation** ($P_{G'|G}^{\text{SP}}$). Each edge in the BA graph G_{ba} and the cycle motif G_c is dropped with probability p , but the edges of the house motif G_h are left unchanged.

To theoretically evaluate the fundamental performance limits of contrastive learning mechanisms under semantics-agnostic and semantics-preserving augmentations, in Appendix A, we introduce the concept of an *empirical contrastive learner* (ECL). At a high level, an ECL aims to assign similar embeddings to graphs that are deemed similar by an underlying distance measure. It first partitions the training set into at most κ clusters based on a distance measure $d(G, G')$, and then assigns embeddings such that graphs within the same cluster have similar embeddings and graphs in different clusters have maximally discriminative embeddings. In our analysis of the BA2-Motifs benchmark, we consider the distance measure $d_c(G, G')$ which is equal to the absolute difference in the number of cycles in graphs G and G' . For instance, $d_c(G_c, G_h) = 2$ since the cycle motif has one cycle and the house motif has three cycles.

The following theorem, whose proof is deferred to Appendix A, shows that under semantics-preserving augmentation $P_{G'|G}^{\text{SP}}$, the ECL can successfully cluster the graphs according to their labels, resulting in zero classification error. In contrast, under semantics-agnostic augmentation $P_{G'|G}^{\text{SA}}$, the ECL fails to cluster the graphs effectively, leading to an error rate close to $\frac{q}{2}$.

THEOREM 1. *In the modified BA-2Motifs classification task described above, consider the ECLs $f_{\text{enc}}^{\text{SA}}$ and $f_{\text{enc}}^{\text{SP}}$ which correspond to the semantic-agnostic augmentation $P_{G'|G}^{\text{SA}}$ and the semantic-preserving augmentation $P_{G'|G}^{\text{SP}}$, respectively, with edge-drop probability $p > 0.3$, and as the size of the unlabeled training set \mathcal{T}_u grows asymptotically large, the following hold:*

- The error rate of an empirical risk minimization (ERM) operating on the embeddings from $f_{\text{enc}}^{\text{SA}}(G)$ converges to $\frac{q}{2}$.
- The error rate of an ERM operating on the embeddings from $f_{\text{enc}}^{\text{SP}}(G)$ converges to 0.

This theorem suggests that semantics-preserving augmentations can endow the ECL with the capability of producing embeddings that facilitate perfect classification in the asymptotic regime, while semantics-agnostic augmentations inevitably lead to significantly higher error rates. Although the theorem is demonstrated on a

benchmark dataset, the underlying principles are potentially extendable to more real-world scenarios, where critical substructures determine graph labels [18, 41, 48].

5 Experiments

In this section, we conduct extensive experiments to evaluate the proposed EPA-GRL method and compare it with the widely used augmentation methods and the SOTA GRL methods.

5.1 Experimental Setup

Datasets. To evaluate the performance of EPA-GRL, we use six benchmark real-world datasets with graph-level labels, including MUTAG [18], Benzene [1], Alkane-Carbonyl [1], Fluoride-Carbonyl [1], D&D [9], and PROTEINS [4, 9]. Among them, MUTAG, Benzene, Alkane-Carbonyl and Fluoride-Carbonyl also provide the ground truth subgraph that explains the classification of every graph instance, *i.e.*, the semantics pattern. This information will be used for our analysis of semantics-preservation. Detailed statistics and descriptions of the datasets can be found in Appendix C.1.

Baselines. The key contribution of this work is a novel graph augmentation method EPA, which is agnostic to the choice of the GRL method. Therefore, in the experiment, we consider two widely used contrastive learning algorithms, *i.e.*, GraphCL [43] and SimSiam [7], as the basic GRL method on augmented graphs, and compare EPA with its semantics-agnostic counterparts (“Vanilla”): (1) *Node-Dropping* randomly removes a portion of nodes and their connections; (2) *Edge-Dropping* perturbs the connectivity in a graph by randomly removing a certain percentage of edges; (3) *Attribute-Masking* randomly masks some node features so that a model can only infer information from the unmasked part of features; (4) *Subgraph-Sample* randomly samples a subgraph using random walk from the original graph as the augmented graph; and (5) *Mixup* combines two pruned graphs to form an augmented graph.

Moreover, we compare our EPA enhanced GRL, namely EPA-GRL, with other SOTA approaches for GRL, including AD-GCL [28], JOAO [42], AutoGCL [40], and SimGRACE [34]. As they are un-/self-supervised methods, we further extend them to semi-supervised methods using a two-step framework proposed in [43]: (1) pretrain a GNN encoder on all unlabeled graphs using each of the aforementioned self-supervised learning methods; (2) fine-tune the GNN encoder with the labeled graphs using cross-entropy loss. In particular, AutoGCL has a design that enables joint training of the two processes. We adopt it for its semi-supervised training.

Implementation. We evaluate the classification performance based on the learned embeddings provided by different GRL methods. Specifically, following [43], after training a GNN by a GRL algorithm, the embeddings generated by the GNN are fed to an SVM for classification. Each dataset is divided into 80%/10%/10% for (disjoint) train/val/test sets. We randomly sample 50 graphs from the training set for training SVM. For semi-supervised GRL methods (including EPA-GRL), the same 50 labeled graphs are used together with the unlabeled graphs in the training set for training GNNs. For unsupervised GRL methods, all graphs in the dataset (without using labels) are used for training GNNs. Here a 3-layer Graph Convolutional Network (GCN) [16] is employed as the backbone GNN for all GRL methods. We also evaluate GIN backbone [39] in Appendix D.1. For

all methods, the GNNs are trained using Adam optimizer [15] with a learning rate of 1×10^{-3} . For our EPA-GRL, a weight decay of 5×10^{-4} is used for training the explainer, and τ in Eq. (3) is set as 0.2. The detailed configurations of the compared GRL methods can be found in Appendix C.2. For the augmentation baselines, Node-Dropping removes 10% nodes; Edge-Dropping perturbs 10% edges; Attribute-Masking masks 10% features; Subgraph-Sample randomly selects half of the nodes from the graph as starting nodes and performs random walks of 10 steps from each; Mix-up prunes 20% of a graph randomly picked in the same batch to form an augmented graph. The implementation details about EPA augmentations are deferred to Appendix B.1. All experiments are performed on a Linux machine with 8 Nvidia A100-PCIE 40GB GPUs, with CUDA version 12.4.

5.2 Experimental Results

5.2.1 Comparing Augmentation Methods. We report the mean accuracy of graph classification over 10 random runs. Table 2 and Table 3 summarize the results of comparing EPA with different augmentation techniques using GraphCL and SimSiam as the GRL framework, respectively. From the results, we have several observations. First, different augmentation techniques may be useful to different extents on different datasets, where the methods modifying graph structures (*e.g.*, Subgraph, Mixup, Edge Dropping, etc.) are generally better than Attribute Masking. This is because structural changes imply more variances on graphs than node features, which is a desideratum for augmenting the dataset. Second, GraphCL generally leads to better performance than SimSiam, suggesting a better fit of GraphCL as a GRL benchmark. Therefore, GraphCL is considered as the default GRL framework in the subsequent experiments unless otherwise stated. Third, in most cases, our method EPA outperform each Vanilla augmentation technique, with up to 7.83% relative improvement (Edge-Dropping on PROTEINS) using GraphCL and 5.98% relative improvement (Subgraph on PROTEINS) using SimSiam, indicating its generalizability across various augmentations and datasets, and its GRL-agnostic design for plug-and-play with different GRL methods. Finally, EPA is less sensitive to the loss of semantics caused by random perturbations, such as the degraded accuracy of Vanilla Node Dropping on MUTAG in Table 2 and Vanilla Edge Dropping/Mixup on PROTEINS in Table 3. This is because the perturbation is constrained to the marginal subgraphs outside the semantic patterns by EPA, leading to its robustness to the potentially arbitrary changes caused by perturbations.

5.2.2 Comparing GRL Methods. In Table 4, we compare EPA-GRL with the SOTA un-/self-supervised and semi-supervised GRL methods, which use a mixture of the aforementioned augmentation methods in the same way as in [43], *i.e.*, randomly choosing an augmentation method for each original graph. All semi-supervised methods are trained using 50 labels. We also include “Supervised” as a baseline where the GNN encoder is only trained with the (small set of) labeled graphs \mathcal{T}_ℓ using cross-entropy loss. We observe that using a few labeled graphs \mathcal{T}_ℓ in “Supervised” achieves competitive performances compared to training with the vast unlabeled graphs. Besides, for each GRL baseline method, its semi-supervised version (“SS-”) is better than its self-supervised version in most cases.

Table 2: Comparison of different graph augmentation methods using GraphCL as the GRL framework.

Augmentation Method		MUTAG	Benzene	Alkane-Car.	Fluoride-Car.	D&D	PROTEINS
Node Dropping	Vanilla	0.803 \pm 0.030	0.767 \pm 0.049	0.965 \pm 0.038	0.648 \pm 0.067	0.653 \pm 0.070	0.728 \pm 0.073
	EPA	0.860 \pm 0.020	0.765 \pm 0.050	0.979 \pm 0.020	0.656 \pm 0.066	0.649 \pm 0.065	0.744 \pm 0.077
Edge Dropping	Vanilla	0.858 \pm 0.027	0.753 \pm 0.043	0.942 \pm 0.047	0.659 \pm 0.044	0.660 \pm 0.048	0.702 \pm 0.077
	EPA	0.861 \pm 0.053	0.754 \pm 0.050	0.948 \pm 0.026	0.662 \pm 0.053	0.665 \pm 0.050	0.757 \pm 0.055
Attribute Masking	Vanilla	0.820 \pm 0.064	0.762 \pm 0.052	0.967 \pm 0.032	0.653 \pm 0.071	0.616 \pm 0.060	0.683 \pm 0.077
	EPA	0.850 \pm 0.047	0.750 \pm 0.032	0.975 \pm 0.027	0.658 \pm 0.046	0.624 \pm 0.048	0.715 \pm 0.057
Subgraph	Vanilla	0.842 \pm 0.038	0.762 \pm 0.034	0.973 \pm 0.027	0.655 \pm 0.044	0.651 \pm 0.060	0.704 \pm 0.077
	EPA	0.846 \pm 0.037	0.765 \pm 0.056	0.987 \pm 0.019	0.644 \pm 0.059	0.663 \pm 0.065	0.728 \pm 0.082
Mixup	Vanilla	0.850 \pm 0.024	0.766 \pm 0.040	0.971 \pm 0.019	0.650 \pm 0.050	0.643 \pm 0.040	0.728 \pm 0.072
	EPA	0.852 \pm 0.027	0.769 \pm 0.061	0.975 \pm 0.020	0.661 \pm 0.060	0.640 \pm 0.032	0.750 \pm 0.066

Table 3: Comparison of different graph augmentation methods using SimSiam as the GRL framework.

Augmentation Method		MUTAG	Benzene	Alkane-Car.	Fluoride-Car.	D&D	PROTEINS
Node Dropping	Vanilla	0.840 \pm 0.042	0.725 \pm 0.061	0.943 \pm 0.026	0.607 \pm 0.040	0.674 \pm 0.036	0.700 \pm 0.060
	EPA	0.855 \pm 0.049	0.730 \pm 0.066	0.945 \pm 0.031	0.637 \pm 0.049	0.676 \pm 0.037	0.731 \pm 0.090
Edge Dropping	Vanilla	0.837 \pm 0.045	0.735 \pm 0.061	0.947 \pm 0.021	0.618 \pm 0.045	0.671 \pm 0.056	0.687 \pm 0.089
	EPA	0.855 \pm 0.051	0.738 \pm 0.073	0.948 \pm 0.030	0.640 \pm 0.043	0.668 \pm 0.031	0.728 \pm 0.076
Attribute Masking	Vanilla	0.840 \pm 0.048	0.715 \pm 0.052	0.947 \pm 0.014	0.610 \pm 0.026	0.649 \pm 0.065	0.726 \pm 0.070
	EPA	0.854 \pm 0.048	0.711 \pm 0.070	0.943 \pm 0.023	0.624 \pm 0.064	0.668 \pm 0.059	0.750 \pm 0.080
Subgraph	Vanilla	0.838 \pm 0.039	0.704 \pm 0.079	0.950 \pm 0.015	0.610 \pm 0.022	0.665 \pm 0.031	0.702 \pm 0.068
	EPA	0.847 \pm 0.052	0.715 \pm 0.088	0.944 \pm 0.021	0.629 \pm 0.047	0.673 \pm 0.074	0.744 \pm 0.084
Mixup	Vanilla	0.829 \pm 0.034	0.729 \pm 0.070	0.945 \pm 0.026	0.620 \pm 0.031	0.654 \pm 0.060	0.700 \pm 0.075
	EPA	0.830 \pm 0.070	0.721 \pm 0.062	0.951 \pm 0.037	0.647 \pm 0.060	0.661 \pm 0.060	0.721 \pm 0.070

Table 4: Comparison of different self-supervised and semi-supervised (denoted as “SS-”) GRL methods.

GRL Method		MUTAG	Benzene	Alkane-Car.	Fluoride-Car.	D&D	PROTEINS
Supervised		0.848 \pm 0.028	0.761 \pm 0.034	0.970 \pm 0.033	0.661 \pm 0.046	0.626 \pm 0.071	0.709 \pm 0.047
Self-Sup.	GraphCL	0.846 \pm 0.032	0.755 \pm 0.046	0.971 \pm 0.019	0.656 \pm 0.081	0.637 \pm 0.065	0.712 \pm 0.050
	AD-GCL	0.854 \pm 0.025	0.722 \pm 0.076	0.942 \pm 0.028	0.656 \pm 0.045	0.622 \pm 0.026	<u>0.736</u> \pm 0.070
	JOAO	0.823 \pm 0.034	0.735 \pm 0.061	0.960 \pm 0.019	0.626 \pm 0.074	<u>0.650</u> \pm 0.074	0.725 \pm 0.067
	AutoGCL	0.812 \pm 0.071	0.759 \pm 0.065	0.912 \pm 0.101	0.610 \pm 0.069	0.631 \pm 0.074	0.722 \pm 0.053
	SimGRACE	0.834 \pm 0.050	0.735 \pm 0.067	0.891 \pm 0.155	0.581 \pm 0.060	0.583 \pm 0.077	0.719 \pm 0.068
Semi-Sup.	SS-GraphCL	0.853 \pm 0.034	<u>0.764</u> \pm 0.054	<u>0.978</u> \pm 0.020	0.658 \pm 0.048	0.639 \pm 0.060	0.720 \pm 0.063
	SS-AD-GCL	<u>0.857</u> \pm 0.036	0.739 \pm 0.046	0.976 \pm 0.021	0.660 \pm 0.053	0.615 \pm 0.057	0.733 \pm 0.061
	SS-JOAO	0.849 \pm 0.038	0.762 \pm 0.047	0.962 \pm 0.022	0.668 \pm 0.033	0.652 \pm 0.076	0.726 \pm 0.063
	SS-AutoGCL	0.824 \pm 0.038	0.750 \pm 0.040	0.970 \pm 0.019	0.615 \pm 0.052	0.639 \pm 0.065	0.734 \pm 0.066
	SS-SimGRACE	0.834 \pm 0.041	0.728 \pm 0.048	0.902 \pm 0.032	0.611 \pm 0.072	0.598 \pm 0.081	0.713 \pm 0.056
	EPA-GRL	0.861 \pm 0.032	0.765 \pm 0.032	0.982 \pm 0.020	<u>0.663</u> \pm 0.028	<u>0.650</u> \pm 0.065	0.744 \pm 0.065

These results suggest the effectiveness of leveraging (a handful of) labels for GRL. Our method EPA-GRL integrates this merit but is remarkably different from the baseline methods which only use labels for updating model parameters. In contrast, EPA-GRL uses the limited amount of labels for structure learning, *i.e.*, explicitly learning the sub-structures that are semantically meaningful. Thus, it achieves substantial performance gains in general, meanwhile maintaining a consistently stable performance with low standard deviations across the datasets.

5.2.3 Ablation Analysis. In this section, we use the MUTAG dataset for performance analysis. To understand EPA’s efficiency in using

labels, we analyze the impacts of the number of labeled graphs for explainer pre-training, *i.e.*, $|\mathcal{T}_\ell|$. We vary $|\mathcal{T}_\ell|$ within $\{50, 100, 150\}$ while fixing the number of training graphs for SVM as 50. Fig. 4 summarizes the results. As $|\mathcal{T}_\ell|$ increases, EPA-GRL gains more accuracy on all augmentation methods. The “Vanilla” methods achieve constant results because they are semantic agnostic. As such, EPA is capable of making effective use of more labels for providing better augmentations. However, as labeling is usually expensive, we restrict most of our experiments to the challenging region with only 50 labeled graphs. Additionally, we evaluate the impacts of varying numbers of labeled graphs for the downstream training of SVM. As shown in Fig. 5, both “Vanilla” and EPA augmented graphs enable

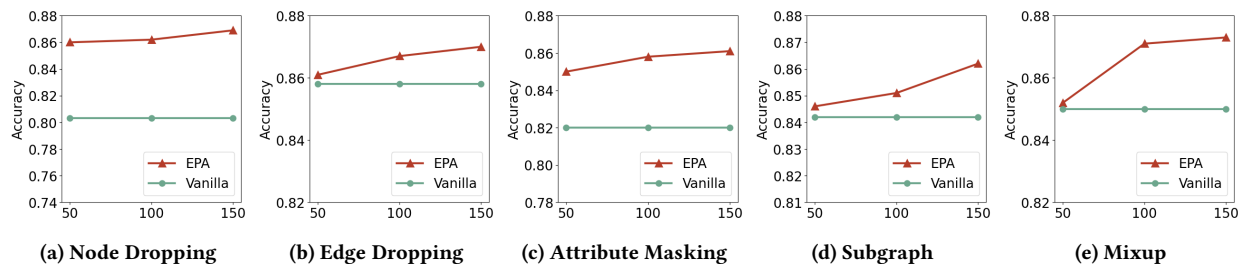


Figure 4: Parameter analysis with different numbers of training samples for pre-training.

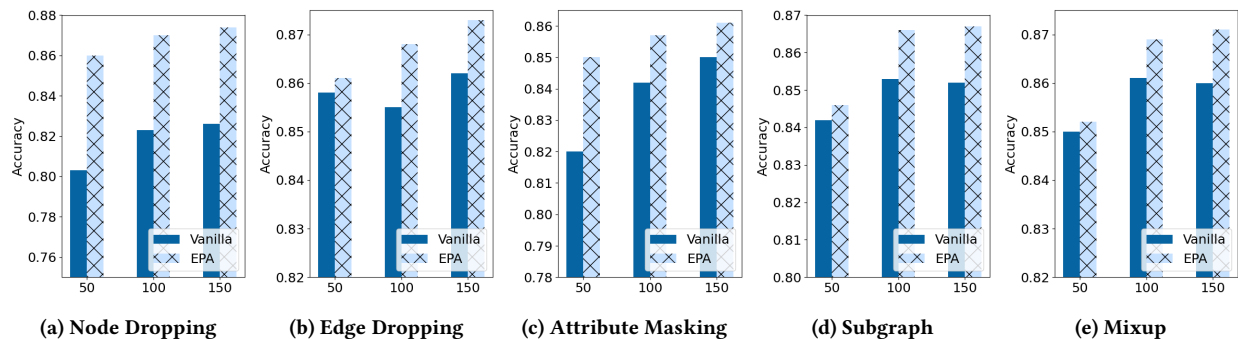


Figure 5: Parameter analysis with different number of training samples for downstream training.

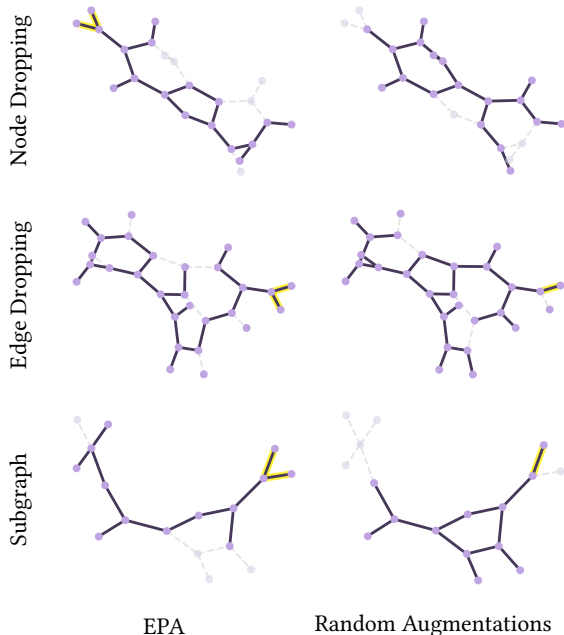


Figure 6: Visualization of the augmented graphs using different methods. Yellow edges highlight the explanatory sub-structures. Gray nodes denote deleted nodes. Dashed edges denote deleted edges.

high-quality graph embeddings for effective downstream training with more and more labels. In particular, EPA-GRL consistently

produce better embeddings than the baseline method as suggested by the clear accuracy gap.

5.3 Case Studies

In this section, we investigate how semantics are preserved by EPA by examining the augmented graphs. Using MUTAG, we visualize the augmented graphs for Node-Dropping, Edge-Dropping, and Subgraph as examples in Fig 6. The ground-truth explanatory sub-structures, *i.e.*, semantic patterns, are highlighted by yellow edges. As can be seen, through the GNN explainer, EPA successfully preserves the explanatory sub-structures meanwhile perturbing the marginal subgraphs (as represented by gray nodes and dashed edges). In contrast, Vanilla augmentations may randomly perturb the explanatory sub-structures, leading to a significant loss of semantics in the augmented graphs. In particular, it drops the entire semantic subgraph by Node Dropping. This result justifies the superior performance of EPA-GRL in Table 2 and Table 3.

5.4 Additional Analysis

In addition to the aforementioned experiments, we provide a visual analysis on the embeddings of EPA on different datasets in Appendix D.3. Moreover, in Appendix D.1, we evaluate our method on two additional datasets (a synthetic dataset and a large real-world dataset) and with GIN [39] as another base GNN model, demonstrating the generalizability of EPA across different datasets and GNN architectures.

6 Related Work

Explainable Graph Neural Networks. Explainability in GNNs has gained significant attention, with various methods proposed to enhance transparency in graph-based tasks [5, 11, 17, 18, 21, 22, 32, 37, 41, 46–49]. They can lead to significant improvements in understanding GNN decision-making processes, enabling explanations at both individual instances [5, 18, 41] and global model levels [25, 32, 46]. Early approaches primarily used gradient-based methods such as Saliency Maps (SA) [3] and Grad-CAM [23] to provide explanations. More recent advancements have introduced model-agnostic techniques, including perturbation-based methods [18, 33], surrogate models [10, 30], and generation-based approaches [24, 32, 46]. Perturbation-based methods, such as GN-Explainer [41] and PGExplainer [18], generate explanations by perturbing graph features or structures to identify the most important components influencing predictions. Surrogate models [30] approximate the original GNN with simpler models to explain local predictions, while generation-based methods [32, 46] leverage generative models to provide both instance-level and model-level explanations. Our work innovatively builds upon these explainability techniques, particularly perturbation-based methods, to guide the augmentation process in graph contrastive learning, ensuring that critical semantic structures are preserved.

Graph Contrastive Learning. Contrastive learning on graphs can be categorized into two different levels of tasks: node-level task [51, 52] and graph-level task [26, 28, 34, 40, 42, 43]. In this study, we focus on graph-level tasks. For example, GraphCL [43] performs graph contrastive learning by utilizing four different data augmentation methods: node dropping, edge dropping, subgraph sampling, and attribute masking; JOAO [42] propose a unified bi-level optimization framework that automatically selects the suitable data augmentation method from GraphCL; AD-GCL [28] utilizes adversarial augmentation methods to prevent GNNs from capturing redundant information from the original graph during training. AutoGCL [40] uses learnable graph view generators guided by an auto augmentation strategy to introduce appropriate augmentation variances during contrastive learning; SimGRACE [34] uses different graph encoders as generators of contrastive graphs and compares the semantic similarity between graphs obtained from the perturbed encoders for contrastive learning. However, unlike our proposed method, these existing approaches do not explicitly consider preserving the semantic information of graphs during the data augmentation process, which may lead to potential loss of critical structural information.

7 Conclusion

In this paper, we study data augmentation methods for graph contrastive learning. The key challenge is that most existing studies focus only on structural perturbations, overlooking the importance of preserving semantic information. To address this, we propose a framework EPA-GRL for graph contrastive learning. We incorporate explanatory information into data augmentation methods and use theoretical analysis and experiments to demonstrate that our method outperforms baseline models across multiple datasets of varying sizes and types, while also being flexible and easy to use.

References

- [1] Chirag Agarwal, Owen Queen, Himabindu Lakkaraju, and Marinka Zitnik. 2023. Evaluating explainability for graph neural networks. *Scientific Data* 10, 1 (2023), 144.
- [2] Réka Albert and Albert-László Barabási. 2002. Statistical mechanics of complex networks. *Reviews of modern physics* 74, 1 (2002), 47.
- [3] Federico Baldassarre and Hossein Azizpour. 2019. Explainability techniques for graph convolutional networks. *arXiv preprint arXiv:1905.13686* (2019).
- [4] Karsten M Borgwardt, Cheng Soon Ong, Stefan Schönauer, SVN Vishwanathan, Alex J Smola, and Hans-Peter Kriegel. 2005. Protein function prediction via graph kernels. *Bioinformatics* 21, suppl_1 (2005), i47–i56.
- [5] Jialin Chen, Shirley Wu, Abhijit Gupta, and Rex Ying. 2024. D4explainer: In-distribution explanations of graph neural network via discrete denoising diffusion. *Advances in Neural Information Processing Systems* 36 (2024).
- [6] Ting Chen, Simon Kornblith, Mohammad Norouzi, and Geoffrey Hinton. 2020. A simple framework for contrastive learning of visual representations. In *International conference on machine learning*. PMLR, 1597–1607.
- [7] Xinlei Chen and Kaiming He. 2021. Exploring simple siamese representation learning. In *Proceedings of the IEEE/CVF conference on computer vision and pattern recognition*. 15750–15758.
- [8] Asim Kumar Debnath, Rosa L Lopez de Compadre, Gargi Debnath, Alan J Shusterman, and Corwin Hansch. 1991. Structure-activity relationship of mutagenic aromatic and heteroaromatic nitro compounds. correlation with molecular orbital energies and hydrophobicity. *Journal of medicinal chemistry* 34, 2 (1991), 786–797.
- [9] Paul D Dobson and Andrew J Doig. 2003. Distinguishing enzyme structures from non-enzymes without alignments. *Journal of molecular biology* 330, 4 (2003), 771–783.
- [10] Alexandre Duval and Fragkiskos D Malliaros. 2021. Graphsvx: Shapley value explanations for graph neural networks. In *Machine Learning and Knowledge Discovery in Databases. Research Track: European Conference, ECML PKDD 2021, Bilbao, Spain, September 13–17, 2021, Proceedings, Part II 21*. Springer, 302–318.
- [11] Junfeng Fang, Xiang Wang, An Zhang, Zemin Liu, Xiangnan He, and Tat-Seng Chua. 2023. Cooperative Explanations of Graph Neural Networks. In *Proceedings of the Sixteenth ACM International Conference on Web Search and Data Mining*. 616–624.
- [12] Kaiming He, Haoqi Fan, Yuxin Wu, Saining Xie, and Ross Girshick. 2020. Momentum contrast for unsupervised visual representation learning. In *Proceedings of the IEEE/CVF conference on computer vision and pattern recognition*. 9729–9738.
- [13] Junzhong Ji, Hao Jia, Yating Ren, and Minglong Lei. 2023. Supervised contrastive learning with structure inference for graph classification. *IEEE Transactions on Network Science and Engineering* 10, 3 (2023), 1684–1695.
- [14] Prannay Khosla, Piotr Teterwak, Chen Wang, Aaron Sarna, Yonglong Tian, Phillip Isola, Aaron Maschiot, Ce Liu, and Dilip Krishnan. 2020. Supervised contrastive learning. *Advances in neural information processing systems* 33 (2020), 18661–18673.
- [15] D Kinga, Jimmy Ba Adam, et al. 2015. A method for stochastic optimization. In *International conference on learning representations (ICLR)*, Vol. 5. San Diego, California, 6.
- [16] Thomas N. Kipf and Max Welling. 2017. Semi-Supervised Classification with Graph Convolutional Networks. In *5th International Conference on Learning Representations, ICLR 2017, Toulon, France, April 24–26, 2017, Conference Track Proceedings*. OpenReview.net. <https://openreview.net/forum?id=SJU4ayYgl>
- [17] Wanyu Lin, Hao Lan, and Baochun Li. 2021. Generative causal explanations for graph neural networks. In *International Conference on Machine Learning*. PMLR, 6666–6679.
- [18] Dongsheng Luo, Wei Cheng, Dongkuan Xu, Wenchao Yu, Bo Zong, Haifeng Chen, and Xiang Zhang. 2020. Parameterized explainer for graph neural network. *Advances in neural information processing systems* 33 (2020), 19620–19631.
- [19] Dongsheng Luo, Tianxiang Zhao, Wei Cheng, Dongkuan Xu, Feng Han, Wenchao Yu, Xiao Liu, Haifeng Chen, and Xiang Zhang. 2024. Towards inductive and efficient explanations for graph neural networks. *IEEE Transactions on Pattern Analysis and Machine Intelligence* (2024).
- [20] Kha-Dinh Luong and Ambuj K Singh. 2024. Fragment-based pretraining and finetuning on molecular graphs. *Advances in Neural Information Processing Systems* 36 (2024).
- [21] Jing Ma, Ruocheng Guo, Saumitra Mishra, Aidong Zhang, and Jundong Li. 2022. Clear: Generative counterfactual explanations on graphs. *Advances in Neural Information Processing Systems* 35 (2022), 25895–25907.
- [22] Siqi Miao, Yunan Luo, Mia Liu, and Pan Li. 2023. Interpretable Geometric Deep Learning via Learnable Randomness Injection. In *Proceedings of the International Conference on Learning Representations (ICLR)*.
- [23] Phillip E Pope, Soheil Kolouri, Mohammad Rostami, Charles E Martin, and Heiko Hoffmann. 2019. Explainability methods for graph convolutional neural networks. In *Proceedings of the IEEE/CVF conference on computer vision and pattern recognition*. 10772–10781.

- [24] Caihua Shan, Yifei Shen, Yao Zhang, Xiang Li, and Dongsheng Li. 2021. Reinforcement learning enhanced explainer for graph neural networks. *Advances in Neural Information Processing Systems* 34 (2021), 22523–22533.
- [25] Yong-Min Shin, Sun-Woo Kim, and Won-Yong Shin. 2024. PAGE: Prototype-Based Model-Level Explanations for Graph Neural Networks. *IEEE Trans. Pattern Anal. Mach. Intell.* 46, 10 (2024), 6559–6576. <https://doi.org/10.1109/TPAMI.2024.3379251>
- [26] Fan-Yun Sun, Jordan Hoffmann, Vikas Verma, and Jian Tang. 2020. InfoGraph: Unsupervised and Semi-supervised Graph-Level Representation Learning via Mutual Information Maximization. In *8th International Conference on Learning Representations, ICLR 2020, Addis Ababa, Ethiopia, April 26–30, 2020*. OpenReview.net. <https://openreview.net/forum?id=r1lff2NYvH>
- [27] Mengying Sun, Jing Xing, Huijun Wang, Bin Chen, and Jiayu Zhou. 2021. MoCL: data-driven molecular fingerprint via knowledge-aware contrastive learning from molecular graph. In *Proceedings of the 27th ACM SIGKDD conference on knowledge discovery & data mining*. 3585–3594.
- [28] Sushel Suresh, Pan Li, Cong Hao, and Jennifer Neville. 2021. Adversarial graph augmentation to improve graph contrastive learning. *Advances in Neural Information Processing Systems* 34 (2021), 15920–15933.
- [29] Yonglong Tian, Chen Sun, Ben Poole, Dilip Krishnan, Cordelia Schmid, and Phillip Isola. 2020. What makes for good views for contrastive learning? *Advances in neural information processing systems* 33 (2020), 6827–6839.
- [30] Minh Vu and My T Thai. 2020. Pgm-explainer: Probabilistic graphical model explanations for graph neural networks. *Advances in neural information processing systems* 33 (2020), 12225–12235.
- [31] Hanchen Wang, Jean Kaddour, Shengchao Liu, Jian Tang, Joan Lasenby, and Qi Liu. 2023. Evaluating Self-Supervised Learning for Molecular Graph Embeddings. In *Advances in Neural Information Processing Systems*, A. Oh, T. Naumann, A. Globerson, K. Saenko, M. Hardt, and S. Levine (Eds.), Vol. 36. Curran Associates, Inc., 68028–68060.
- [32] Xiaoqi Wang and Han-Wei Shen. 2023. GNNInterpreter: A Probabilistic Generative Model-Level Explanation for Graph Neural Networks. In *The Eleventh International Conference on Learning Representations, ICLR 2023, Kigali, Rwanda, May 1–5, 2023*. OpenReview.net. <https://openreview.net/forum?id=rqq6Dh8t4d>
- [33] Xiang Wang, Yingxin Wu, An Zhang, Xiangnan He, and Tat-Seng Chua. 2021. Towards multi-grained explainability for graph neural networks. *Advances in Neural Information Processing Systems* 34 (2021), 18446–18458.
- [34] Jun Xia, Lirong Wu, Jintao Chen, Bozhen Hu, and Stan Z Li. 2022. Simgrace: A simple framework for graph contrastive learning without data augmentation. In *Proceedings of the ACM Web Conference 2022*. 1070–1079.
- [35] Teng Xiao, Huaisheng Zhu, Zhengyu Chen, and Suhang Wang. 2023. Simple and Asymmetric Graph Contrastive Learning without Augmentations. In *Advances in Neural Information Processing Systems*, A. Oh, T. Naumann, A. Globerson, K. Saenko, M. Hardt, and S. Levine (Eds.), Vol. 36. Curran Associates, Inc., 16129–16152.
- [36] Teng Xiao, Huaisheng Zhu, Zhiwei Zhang, Zhimeng Guo, Charu C. Aggarwal, Suhang Wang, and Vasant G Honavar. 2024. Efficient Contrastive Learning for Fast and Accurate Inference on Graphs. In *Forty-first International Conference on Machine Learning*.
- [37] Yaochen Xie, Sumeet Katariya, Xianfeng Tang, Edward Huang, Nikhil Rao, Karthik Subbian, and Shuiwang Ji. 2022. Task-agnostic graph explanations. *Advances in Neural Information Processing Systems* 35 (2022), 12027–12039.
- [38] Dongkuan Xu, Wei Cheng, Dongsheng Luo, Haifeng Chen, and Xiang Zhang. 2021. Infogcl: Information-aware graph contrastive learning. *Advances in Neural Information Processing Systems* 34 (2021), 30414–30425.
- [39] Keyulu Xu, Weihua Hu, Jure Leskovec, and Stefanie Jegelka. 2019. How Powerful are Graph Neural Networks?. In *7th International Conference on Learning Representations, ICLR 2019, New Orleans, LA, USA, May 6–9, 2019*.
- [40] Yihang Yin, Qingzhong Wang, Siyu Huang, Haoyi Xiong, and Xiang Zhang. 2022. Autogcl: Automated graph contrastive learning via learnable view generators. In *Proceedings of the AAAI conference on artificial intelligence*, Vol. 36. 8892–8900.
- [41] Zhitao Ying, Dylan Bourgeois, Jiaxuan You, Marinka Zitnik, and Jure Leskovec. 2019. Gnnexplainer: Generating explanations for graph neural networks. *Advances in neural information processing systems* 32 (2019).
- [42] Yuning You, Tianlong Chen, Yang Shen, and Zhangyang Wang. 2021. Graph contrastive learning automated. In *International Conference on Machine Learning*. PMLR, 12121–12132.
- [43] Yuning You, Tianlong Chen, Yongduo Sui, Ting Chen, Zhangyang Wang, and Yang Shen. 2020. Graph Contrastive Learning with Augmentations. In *Advances in Neural Information Processing Systems*, H. Larochelle, M. Ranzato, R. Hadsell, M.F. Balcan, and H. Lin (Eds.), Vol. 33. Curran Associates, Inc., 5812–5823.
- [44] Yuning You, Tianlong Chen, Zhangyang Wang, and Yang Shen. 2022. Bringing your own view: Graph contrastive learning without prefabricated data augmentations. In *Proceedings of the fifteenth ACM international conference on web search and data mining*. 1300–1309.
- [45] Junchi Yu, Tingyang Xu, Yu Rong, Yatao Bian, Junzhou Huang, and Ran He. 2021. Graph Information Bottleneck for Subgraph Recognition. In *9th International Conference on Learning Representations, ICLR 2021, Virtual Event, Austria, May 3–7, 2021*. OpenReview.net. <https://openreview.net/forum?id=bM4Iqfg8M2k>
- [46] Hao Yuan, Jiliang Tang, Xia Hu, and Shuiwang Ji. 2020. Xgnn: Towards model-level explanations of graph neural networks. In *Proceedings of the 26th ACM SIGKDD international conference on knowledge discovery & data mining*. 430–438.
- [47] Hao Yuan, Haiyang Yu, Shurui Gui, and Shuiwang Ji. 2022. Explainability in graph neural networks: A taxonomic survey. *IEEE transactions on pattern analysis and machine intelligence* 45, 5 (2022), 5782–5799.
- [48] Hao Yuan, Haiyang Yu, Jie Wang, Kang Li, and Shuiwang Ji. 2021. On explainability of graph neural networks via subgraph explorations. In *International conference on machine learning*. PMLR, 12241–12252.
- [49] Xu Zheng, Farhad Shirani, Tianchun Wang, Wei Cheng, Zhuomin Chen, Haifeng Chen, Hua Wei, and Dongsheng Luo. 2024. Towards Robust Fidelity for Evaluating Explainability of Graph Neural Networks. In *The Twelfth International Conference on Learning Representations, ICLR 2024, Vienna, Austria, May 7–11, 2024*. OpenReview.net. <https://openreview.net/forum?id=up6hr4hIQH>
- [50] Yanqiao Zhu, Yichen Xu, Qiang Liu, and Shu Wu. 2021. An Empirical Study of Graph Contrastive Learning. In *NeurIPS Datasets and Benchmarks*. <https://datasets-benchmarks-proceedings.neurips.cc/paper/2021/hash/0e01938fc48a2cfb5f2217fbfb00722d-Abstract-round2.html>
- [51] Yanqiao Zhu, Yichen Xu, Feng Yu, Qiang Liu, Shu Wu, and Liang Wang. 2020. Deep graph contrastive representation learning. *arXiv preprint arXiv:2006.04131* (2020).
- [52] Yanqiao Zhu, Yichen Xu, Feng Yu, Qiang Liu, Shu Wu, and Liang Wang. 2021. Graph contrastive learning with adaptive augmentation. In *Proceedings of the web conference 2021*. 2069–2080.

A Detailed Theoretical Analysis

In this section, we provide the formal definitions and proofs that support our theoretical analysis presented in Sec. 4.

A.1 Definition of the Empirical Contrastive Learner

At a high level, contrastive learning models cluster the set of all possible input graphs into positive and negative pairs, and consequently train a network such that the embeddings of positive pairs are as similar as possible while ensuring that negative pairs are assigned maximally discriminative embeddings. Due to the nature of augmentations, different input graphs can yield augmented graphs that are close or similar to each other, resulting in a situation where a given graph could simultaneously be categorized as both positive and negative relative to another graph. It is tempting to define the ECL to empirically count the number of times two graphs are paired as positives and the number of times they are paired as negatives, assigning identical or discriminative embeddings based on which count is greater. However, this introduces a circular problem: for example, if graph G is more positively paired than negatively paired with both graphs G' and G'' , then we assign similar embeddings to all three. However, if G' and G'' are more negatively paired than positively paired, this assignment becomes inconsistent. Consequently, we define the ECL as an algorithm that considers all possible partitions of the set of graphs. Each partition is assigned a score based on the number of positive pairs within elements of the same subset of the partition, minus the number of negative pairs. The ECL then outputs embeddings based on the highest-scoring partition, with elements of the same subset receiving similar embeddings.

Given a training set¹ $\mathcal{T}_u = \{G_i, i \in [n]\}$ and augmentation mapping $P_{G'|G}$, the augmented set $\mathcal{A} = \{(G_{i,1}, G_{i,2}), i \in [n]\}$ consists of pairs $(G_{i,1}, G_{i,2})$ generated independently based on $P_{G'|G}(\cdot|G_i)$. We define a distance measure $d(G, G') \in \mathbb{R}_{\geq 0}$ between pairs of graphs. The ECL assigns similar embeddings to graphs whose augmentations have a small distance. This is formalized as below.

DEFINITION 1 (EMPIRICAL CONTRASTIVE LEARNER). *Let $P_{G'|G}$ be an augmentation mapping, $d(\cdot, \cdot)$ be a distance measure, and $\kappa > 0$ be a clustering coefficient. For a threshold $\epsilon > 0$, and an arbitrary pair of graphs G, G' , their pairwise score is defined as:*

$$s_\epsilon(G, G') = |\{G_i \in \mathcal{T}_u | d(G, G_{i,1}) < \epsilon, d(G', G_{i,2}) < \epsilon\}| \\ - |\{G_i \in \mathcal{T}_u | d(G, G_{i,1}) < \epsilon, d(G', G_{i,2}) > \epsilon\}|,$$

and their symmetric score is $\bar{s}_\epsilon(G, G') = s_\epsilon(G, G') + s_\epsilon(G', G)$. Let \mathcal{P} denote the set of all possible partitions of \mathcal{T}_u . Then, for $\mathcal{P} \in \mathcal{P}$, let the partition elements corresponding to \mathcal{P} be denoted by $\mathcal{G}_1, \mathcal{G}_2, \dots, \mathcal{G}_{|\mathcal{P}|}$. The partition score is defined as:

$$\pi_\epsilon(\mathcal{P}) = \sum_{i=1}^{|\mathcal{P}|} \sum_{G, G' \in \mathcal{G}_i} \bar{s}_\epsilon(G, G').$$

The empirically optimal κ -partition \mathcal{P}^* is defined as the one with the highest partition score among all elements of \mathcal{P} with size at most κ .

¹Note that in practice, one could also reuse the labeled training set elements \mathcal{T}_l in training the contrastive learning model.

Then, the ECL is defined as follows:

$$f_{\text{enc}}(G) = \mathbf{Z}_{\mathcal{G}^*}(G), \quad \mathcal{G}^*(G) = \arg \max_{\mathcal{G}_i^* \in \mathcal{P}^*} \frac{1}{|\mathcal{G}_i^*|} \sum_{G' \in \mathcal{G}_i^*} \bar{s}_\epsilon(G, G'),$$

where $\mathbf{Z}_{\mathcal{G}^*}, \mathcal{G}^* \in \mathcal{P}^*$ are maximally distinct and normalized vectors².

The ECL assigns embeddings to graphs based on the frequency of positive and negative pairings induced by the augmentation process. It seeks a partition of the graph dataset that maximizes the alignment of positive pairs within the same cluster while separating negative pairs into different clusters.

A.2 Refined Statement and Proof of Theorem 1

Building upon the formal definition of the ECL, we now present a refined statement of Theorem 1, providing precise conditions and outcomes.

THEOREM 2. *In the modified BA2-Motifs classification task described in the prequel, consider the pair of ECLs $f_{\text{enc}}^{\text{sa}}$ and $f_{\text{enc}}^{\text{sp}}$ characterized by $(P_{G'|G}^{\text{sa}}, d_c(G, G'), \kappa, \epsilon)$ and $(P_{G'|G}^{\text{sp}}, d_c(G, G'), \kappa, \epsilon)$, respectively, with edge-drop probability $p > 0.3$, clustering coefficient $\kappa = 2$, and threshold $\epsilon < 1$. As the size of the training set \mathcal{T}_u grows asymptotically large, the following hold:*

- i) The error rate of an ERM operating on $f_{\text{enc}}^{\text{sa}}(G)$ converges to $\frac{q}{2}$.
- ii) The error rate of an ERM operating on $f_{\text{enc}}^{\text{sp}}(G)$ converges to 0.

A.3 Proof of Theorem 2

We note that the application of edge-drop augmentation to the two classes of graphs yields a graph with either 0, 1 or 3 cycles. The reason is that the BA graph itself does not have any cycles, and the house motif originally has 3 cycles, which may produce 0, 1 or 3 cycles after edge-drop, and the cycle motif originally has 1 cycle and may produce 0 or 1 cycle after edge drop. Let $C_i, i \in \{0, 1, 3\}$ represent the collection of all graphs with i cycles. Then, there are four possible partitions with size less than or equal to $\kappa = 2$:

$$\mathcal{P}_1 = \{\{C_0, C_1, C_3\}\}, \\ \mathcal{P}_2 = \{\{C_0, C_1\}, \{C_3\}\}, \\ \mathcal{P}_3 = \{\{C_0\}, \{C_1, C_3\}\}, \\ \mathcal{P}_4 = \{\{C_1\}, \{C_0, C_3\}\}.$$

We evaluate the partition score for each of these partitions under the $P_{G'|G}^{\text{sa}}$ and $P_{G'|G}^{\text{sp}}$ augmentations, to find the highest scoring partition produced by the corresponding ECL, which in turn determined the ERM accuracy.

Case 1: Semantic-Agnostic Augmentations. Recall that $\mathcal{T}_u = \{G_i | i \in [|\mathcal{T}_u|]\}$ represents the training set and $\mathcal{A} = \{(G_{i,1}, G_{i,2}) | i \in [|\mathcal{T}_u|]\}$ represents the augmented pair of graphs. Let $\omega_{k,\ell}, k, \ell \in \{0, 1, 3\}$ be the fraction of augmented pairs $(G_{i,1}, G_{i,2})$ with k and ℓ

²A collection of vectors $\mathbf{z}_i, i \in [m]$ are called maximally distinct and normalized if each vector is normalized, i.e., $|\mathbf{z}_i| = 1$ for all i , and the minimum pairwise Euclidean distance between any two distinct vectors is maximized.

cycles, respectively. Then,

$$\begin{aligned}
G, G' \in C_0 &\Rightarrow \bar{S}_{0,0} \triangleq \bar{s}_\epsilon(G, G') = 2|\mathcal{T}_u|(\omega_{0,0} - \omega_{0,1} - \omega_{0,3}) \\
G, G' \in C_1 &\Rightarrow \bar{S}_{1,1} \triangleq \bar{s}_\epsilon(G, G') = 2|\mathcal{T}_u|(\omega_{1,1} - \omega_{0,1} - \omega_{1,3}) \\
G, G' \in C_3 &\Rightarrow \bar{S}_{3,3} \triangleq \bar{s}_\epsilon(G, G') = 2|\mathcal{T}_u|(\omega_{3,3} - \omega_{0,3} - \omega_{1,3}) \\
G \in C_0, G' \in C_1 &\Rightarrow \bar{S}_{0,1} \triangleq \bar{s}_\epsilon(G, G') \\
&= |\mathcal{T}_u|(2\omega_{0,1} - \omega_{0,0} - \omega_{0,3} - \omega_{1,1} - \omega_{1,3}) \\
G \in C_0, G' \in C_3 &\Rightarrow \bar{S}_{0,3} \triangleq \bar{s}_\epsilon(G, G') \\
&= |\mathcal{T}_u|(2\omega_{0,3} - \omega_{0,0} - \omega_{0,1} - \omega_{1,3} - \omega_{3,3}) \\
G \in C_1, G' \in C_3 &\Rightarrow \bar{S}_{1,3} \triangleq \bar{s}_\epsilon(G, G') \\
&= |\mathcal{T}_u|(2\omega_{1,3} - \omega_{0,1} - \omega_{1,1} - \omega_{0,3} - \omega_{3,3})
\end{aligned}$$

Furthermore:

$$\begin{aligned}
\pi_{\mathcal{P}_1} &= 2(\bar{S}_{0,0} + \bar{S}_{0,1} + \bar{S}_{0,3} + \bar{S}_{1,1} + \bar{S}_{1,3} + \bar{S}_{3,3}), \\
\pi_{\mathcal{P}_2} &= 2(\bar{S}_{0,0} + \bar{S}_{0,1} + \bar{S}_{1,1} + \bar{S}_{3,3}) \\
\pi_{\mathcal{P}_3} &= 2(\bar{S}_{0,0} + \bar{S}_{1,1} + \bar{S}_{1,3} + \bar{S}_{3,3}), \\
\pi_{\mathcal{P}_4} &= 2(\bar{S}_{1,1} + \bar{S}_{0,0} + \bar{S}_{0,3} + \bar{S}_{3,3}).
\end{aligned}$$

Note that the term $\bar{S}_{0,0} + \bar{S}_{1,1} + \bar{S}_{3,3}$ is shared among all the partition scores and does not affect the choice of optimal partition. So, we focus on $\bar{S}_{0,1}$, $\bar{S}_{0,3}$ and $\bar{S}_{1,3}$ terms. Following standard combinatorial arguments, we note that:

$$\begin{aligned}
\mathbb{E}(\omega_{0,0}) &= \frac{1-q}{2} + \frac{q}{2}(1 - (1-p)^5)^2 + \frac{1}{2}(p(1 - (1-p)^5) \\
&\quad + (1-p)(1 - (1-p)^2)(1 - (1-p)^3))^2 \\
\mathbb{E}(\omega_{0,1}) &= \frac{q}{2}(1 - (1-p)^5)(1-p)^5 \\
&\quad + \frac{1}{2}(p((1-p)^5) + ((1-p)^4)(1 - (1-p)^2) \\
&\quad + ((1-p)^3)(1 - (1-p)^3))(p(1 - (1-p)^5) \\
&\quad + (1-p)(1 - (1-p)^2)(1 - (1-p)^3)) \\
\mathbb{E}(\omega_{1,1}) &= \frac{q}{2}((1-p)^5)^2 + \frac{1}{2}(p((1-p)^5) + ((1-p)^4)(1 - (1-p)^2) \\
&\quad + ((1-p)^3)(1 - (1-p)^3))^2 \\
\mathbb{E}(\omega_{1,3}) &= \frac{1}{2}(p((1-p)^5) + ((1-p)^4)(1 - (1-p)^2) \\
&\quad + ((1-p)^3)(1 - (1-p)^3))((1-p)^6) \\
\mathbb{E}(\omega_{0,3}) &= \frac{1}{2}((1-p)^6)(p(1 - (1-p)^5) \\
&\quad + (1-p)(1 - (1-p)^2)(1 - (1-p)^3)) \\
\mathbb{E}(\omega_{3,3}) &= \frac{1}{2}((1-p)^6)^2
\end{aligned}$$

Numerical evaluation yields $0 > \mathbb{E}(\bar{S}_{1,3}) > \max(\mathbb{E}(\bar{S}_{0,1}), \mathbb{E}(\bar{S}_{0,3}))$ for $p > 0.3$. Consequently, using Hoeffding's inequality, we conclude that \mathcal{P}_3 has the highest partition score among the four partitions $\mathcal{P}_i, i \in [4]$ with probability approaching one as $|\mathcal{T}_u| \rightarrow \infty$. As a result, graphs belonging to C_1 and C_3 are assigned the same embedding by the ECL. Consequently, the ERM is unable to distinguish between graphs with 1 and 3 cycles, e.g., graphs with house or cycle motifs. Thus, it achieves a probability of error at least equal to $\frac{q}{2}$.

Case 2: Semantic Preserving Augmentations. Semantic preserving augmentations do not change the number of cycles in the input graph if the graph is attached to a house motif. Consequently,

$$\mathbb{E}(\omega_{0,1}) > 0, \quad \mathbb{E}(\omega_{0,3}) = \mathbb{E}(\omega_{1,3}) = 0.$$

As a result, $0 > \mathbb{E}(\bar{S}_{0,1}) > \max(\mathbb{E}(\bar{S}_{0,3}), \mathbb{E}(\bar{S}_{1,3}))$. The partition \mathcal{P}_2 receives the highest score. So, graphs with 0 or 1 cycles are mapped to the same embedding and graphs with 3 cycles are mapped to a different embedding. Thus, an ERM applied to the output of the ECL achieves zero error rate.

Algorithm 1 Explanation-Preserving Node Dropping

Input: Graph $G = (\mathcal{V}, \mathcal{E})$, trained GNN explainer $\Psi(\cdot)$, dropping ratio p

Output: Explanation-preserving augmented Graph G'

- 1: $G^{(\text{exp})} = \Psi(G)$ ▷ Extract explanation subgraph
 - 2: $\Delta G = G \setminus G^{(\text{exp})} = (\Delta\mathcal{V}, \Delta\mathcal{E})$ ▷ Compute marginal subgraph
 - 3: $\mathcal{V}^{(\text{smp})} = \{v \mid v \in \Delta\mathcal{V}, \text{Bernoulli}(1-p) = 1\}$ ▷ Sample nodes with probability $1-p$
 - 4: $\mathcal{E}^{(\text{smp})} = \{(u, v) \mid (u, v) \in \Delta\mathcal{E}, u \in \mathcal{V}^{(\text{smp})}, v \in \mathcal{V}^{(\text{smp})}\}$ ▷ Keep edges between sampled nodes
 - 5: $G^{(\text{smp})} = (\mathcal{V}^{(\text{smp})}, \mathcal{E}^{(\text{smp})})$ ▷ Construct sampled subgraph
 - 6: $G' = G^{(\text{exp})} \cup G^{(\text{smp})}$ ▷ Combine explanation and sampled subgraphs
 - 7: **return** G'
-

B Detailed Algorithms

B.1 Explanation-Preserving Augmentation Algorithms

In this section, we provide the detailed pseudo code of the proposed explanation-preserving augmentation algorithms.

Explanation-Preserving Node Dropping. Algorithm 1 outlines the process of explanation-preserving node dropping. Given an input graph G , a trained GNN explainer $\Psi(\cdot)$, and a dropping ratio p , the algorithm first extracts the explanation subgraph $G^{(\text{exp})}$ using the explainer. It then identifies the marginal subgraph ΔG by subtracting $G^{(\text{exp})}$ from G . Nodes in ΔG are sampled with probability $1-p$, and edges connecting these sampled nodes are retained. The algorithm constructs a sampled subgraph $G^{(\text{smp})}$ from these nodes and edges. Finally, it combines $G^{(\text{exp})}$ and $G^{(\text{smp})}$ to create the augmented graph G' .

Explanation-Preserving Edge Dropping. Algorithm 2 describes the explanation-preserving edge dropping process. Similar to node dropping, it starts by extracting the explanation subgraph $G^{(\text{exp})}$ and identifying the marginal subgraph ΔG . However, instead of sampling nodes, this algorithm samples edges from ΔG with probability $1-p$. It then collects all nodes that are incident to the sampled edges. The sampled subgraph $G^{(\text{smp})}$ is constructed from these edges and their associated nodes. Finally, we combine $G^{(\text{exp})}$ and $G^{(\text{smp})}$ to produce the augmented graph G' . Explanation-Preserving Node/Edge Dropping preserves the critical node/edge structure identified by the explainer while introducing variability in the connectivity of less important parts of the graph.

Algorithm 2 Explanation-Preserving Edge Dropping

Input: Graph $G = (\mathcal{V}, \mathcal{E})$, trained GNN explainer $\Psi(\cdot)$, dropping ratio p

Output: Explanation-preserving augmented Graph G'

- 1: $G^{(\text{exp})} = \Psi(G)$ ▷ Extract explanation subgraph
- 2: $\Delta G = G \setminus G^{(\text{exp})} = (\Delta\mathcal{V}, \Delta\mathcal{E})$ ▷ Compute marginal subgraph
- 3: $\mathcal{E}^{(\text{smp})} = \{e \mid e \in \Delta\mathcal{E}, \text{Bernoulli}(1-p) = 1\}$ ▷ Sample edges with probability $1-p$
- 4: $\mathcal{V}^{(\text{smp})} = \{v \mid v \in \Delta\mathcal{V}, \exists e \in \mathcal{E}^{(\text{smp})}, v \in e\}$ ▷ Collect nodes of sampled edges
- 5: $G^{(\text{smp})} = (\mathcal{V}^{(\text{smp})}, \mathcal{E}^{(\text{smp})})$ ▷ Construct sampled subgraph
- 6: $G' = G^{(\text{exp})} \cup G^{(\text{smp})}$ ▷ Combine explanation and sampled subgraphs
- 7: **return** G'

Algorithm 3 Explanation-Preserving Attribute Masking

Input: Graph $G = \{\mathcal{V}, \mathcal{E}, \mathbf{X}\}$, trained GNN explainer $\Psi(\cdot)$, masking ratio p

Output: Explanation-preserving augmented Graph G'

- 1: $G^{(\text{exp})} = \Psi(G)$ ▷ Extract explanation subgraph
- 2: $\Delta G = G \setminus G^{(\text{exp})} = (\Delta\mathcal{V}, \Delta\mathcal{E}, \Delta\mathbf{X})$ ▷ Compute marginal subgraph
- 3: $\mathbf{M}^{(\text{smp})} \in \{0, 1\}^{|\Delta\mathcal{V}| \times d_n}$, $m_{ij}^{(\text{smp})} \sim \text{Bernoulli}(1-p)$ ▷ Generate binary mask matrix
- 4: $\mathbf{X}^{(\text{smp})} = \Delta\mathbf{X} \odot \mathbf{M}^{(\text{smp})}$ ▷ Apply pointwise product
- 5: $G^{(\text{smp})} = (\Delta\mathcal{V}, \Delta\mathcal{E}, \mathbf{X}^{(\text{smp})})$ ▷ Construct sampled subgraph
- 6: $G' = G^{(\text{exp})} \cup G^{(\text{smp})}$ ▷ Combine explanation and sampled subgraphs
- 7: **return** G'

Explanation-Preserving Attribute Masking. Algorithm 3 presents the explanation-preserving attribute masking procedure. As with the previous methods, it begins by extracting the explanation subgraph $G^{(\text{exp})}$ and identifying the marginal subgraph ΔG . The key difference lies in the treatment of node features. The algorithm generates a binary mask matrix $\mathbf{M}^{(\text{smp})}$ where each entry is sampled from a Bernoulli distribution with probability $1-p$. This mask is then applied to the feature matrix $\Delta\mathbf{X}$ of the marginal subgraph through a pointwise product operation. The resulting $\mathbf{X}^{(\text{smp})}$ contains masked features for the non-critical nodes. The algorithm constructs $G^{(\text{smp})}$ using the original structure of ΔG but with the masked features. Finally, it combines $G^{(\text{exp})}$ and $G^{(\text{smp})}$ to create G' . This approach maintains the critical node attributes identified by the explainer while introducing controlled noise in the features of less important nodes.

Explanation-Preserving Subgraph. Algorithm 4 details the explanation preserving subgraph sampling process. After extracting the explanation subgraph $G^{(\text{exp})}$ and identifying the marginal subgraph ΔG , the algorithm performs a random walk on ΔG . It starts by randomly selecting an initial node v_0 from ΔG . The algorithm then iteratively expands the sampled node set $\mathcal{V}^{(\text{smp})}$ by randomly selecting nodes from the neighborhood of previously sampled nodes.

Algorithm 4 Explanation-Preserving Subgraph

Input: Graph $G = (\mathcal{V}, \mathcal{E})$, trained GNN explainer $\Psi(\cdot)$, sampling ratio p

Output: Explanation-preserving augmented Graph G'

- 1: $G^{(\text{exp})} = \Psi(G)$ ▷ Extract explanation subgraph
- 2: $\Delta G = G \setminus G^{(\text{exp})} = (\Delta\mathcal{V}, \Delta\mathcal{E})$ ▷ Compute marginal subgraph
- 3: $v_0 \leftarrow$ Random node from $\Delta\mathcal{V}$
- 4: $\mathcal{V}^{(\text{smp})} \leftarrow v_0$
- 5: $\mathcal{V}^{(\text{neigh})} \leftarrow \mathcal{N}(v_0)$ ▷ Get neighbors of v_0
- 6: **while** $|\mathcal{V}^{(\text{smp})}| < p|\Delta\mathcal{V}|$ **do**
- 7: $v \leftarrow$ Random node from $\mathcal{V}^{(\text{neigh})} \setminus \mathcal{V}^{(\text{smp})}$
- 8: $\mathcal{V}^{(\text{smp})} \leftarrow \mathcal{V}^{(\text{smp})} \cup \{v\}$
- 9: $\mathcal{V}^{(\text{neigh})} \leftarrow \mathcal{V}^{(\text{neigh})} \cup (\mathcal{N}(v) \setminus \mathcal{V}^{(\text{smp})})$
- 10: **end while**
- 11: $\mathcal{E}^{(\text{smp})} \leftarrow \{(u, v) \mid (u, v) \in \Delta\mathcal{E}, u \in \mathcal{V}^{(\text{smp})} \text{ or } v \in \mathcal{V}^{(\text{smp})}\}$
- 12: $G^{(\text{smp})} = (\mathcal{V}^{(\text{smp})}, \mathcal{E}^{(\text{smp})})$ ▷ Construct sampled subgraph
- 13: $G' = G^{(\text{exp})} \cup G^{(\text{smp})}$ ▷ Combine explanation and sampled subgraphs
- 14: **return** G'

This process continues until the desired number of nodes (determined by the sampling ratio p) is reached. The algorithm then collects all edges that have at least one endpoint in $\mathcal{V}^{(\text{smp})}$ to form $\mathcal{E}^{(\text{smp})}$. The sampled subgraph $G^{(\text{smp})}$ is constructed from these nodes and edges. Finally, $G^{(\text{exp})}$ and $G^{(\text{smp})}$ are combined to create the augmented graph G' .

Explanation-Preserving Mixup. Algorithm 5 describes the explanation preserving mixup process. This method begins by extracting the explanation subgraph $G^{(\text{exp})}$ from the input graph G and identifying its marginal subgraph ΔG . It then randomly selects another graph G' from the set of available graphs \mathcal{G} and computes its marginal subgraph $\Delta G'$. The algorithm proceeds to mix these marginal subgraphs based on their relative sizes. If ΔG is smaller or equal in size to $\Delta G'$, it samples nodes from $\Delta G'$ to match ΔG 's size and creates a one-to-one mapping between their nodes. If ΔG is larger, it samples a subset of ΔG to match $\Delta G'$'s size, maps these nodes, and retains the unmapped portion of ΔG . The algorithm then constructs edges for the sampled nodes based on the original connections in $\Delta G'$. Finally, it combines the explanation subgraph $G^{(\text{exp})}$ with the mixed marginal subgraph to create the augmented graph $G^{(\text{aug})}$.

Algorithm 5 Explanation-Preserving Mixup

Input: Graph $G = (\mathcal{V}, \mathcal{E})$, a set of graphs \mathcal{G} , trained GNN explainer $\Psi(\cdot)$

Output: Explanation-preserving augmented Graph G'

```

1:  $G^{(\text{exp})} = \Psi(G)$   $\triangleright$  Extract explanation subgraph from  $G$ 
2:  $\Delta G = G \setminus G^{(\text{exp})} = (\Delta\mathcal{V}, \Delta\mathcal{E})$   $\triangleright$  Compute marginal subgraph of  $G$ 
3:  $\tilde{G} = (\tilde{\mathcal{V}}, \tilde{\mathcal{E}}) \leftarrow$  Random graph from  $\mathcal{G}$   $\triangleright$  Sample a random graph
4:  $\Delta\tilde{G} = \tilde{G} - \tilde{G}^{(\text{exp})} = (\Delta\tilde{\mathcal{V}}, \Delta\tilde{\mathcal{E}})$   $\triangleright$  Compute marginal subgraph of  $\tilde{G}$ 
5: if  $|\Delta\mathcal{V}| \leq |\Delta\tilde{\mathcal{V}}|$  then
6:    $\mathcal{V}^{(\text{smp})} \leftarrow$  Random sample of  $|\Delta\mathcal{V}|$  nodes from  $\Delta\tilde{\mathcal{V}}$ 
7:    $f_{\text{map}} : \Delta\mathcal{V} \rightarrow \mathcal{V}^{(\text{smp})}$   $\triangleright$  One-to-one mapping
8:    $\mathcal{E}^{(\text{smp})} = \{(f(u), f(v)) \mid (u, v) \in \Delta\tilde{\mathcal{E}}, u, v \in \mathcal{V}^{(\text{smp})}\}$ 
9:    $G^{(\text{smp})} = (\mathcal{V}^{(\text{smp})}, \mathcal{E}^{(\text{smp})})$ 
10: else
11:    $\mathcal{V}^{(\text{mix})} \leftarrow$  Random sample of  $|\Delta\tilde{\mathcal{V}}|$  nodes from  $\Delta\mathcal{V}$ 
12:    $f_{\text{map}} : \mathcal{V}^{(\text{mix})} \rightarrow \Delta\tilde{\mathcal{V}}$   $\triangleright$  One-to-one mapping for subset
13:    $\mathcal{E}^{(\text{mix})} = \{(f(u), f(v)) \mid (u, v) \in \Delta\tilde{\mathcal{E}}, u, v \in \mathcal{V}^{(\text{mix})}\}$ 
14:    $\mathcal{V}^{(\text{unmix})} = \Delta\mathcal{V} - \mathcal{V}^{(\text{mix})}$ 
15:    $\mathcal{E}^{(\text{unmix})} = \{(u, v) \mid (u, v) \in \Delta\mathcal{E}, u, v \in \mathcal{V}^{(\text{unmix})}\}$ 
16:    $G^{(\text{smp})} = (\mathcal{V}^{(\text{mix})} \cup \mathcal{V}^{(\text{unmix})}, \mathcal{E}^{(\text{mix})} \cup \mathcal{E}^{(\text{unmix})})$ 
17: end if
18:  $G' = G^{(\text{exp})} \cup G^{(\text{smp})}$   $\triangleright$  Combine explanation and sampled subgraphs
19: return  $G'$ 

```

B.2 Graph Representation Learning with Explanation-Preserving Augmentations

Algorithm 6 presents the process of GraphRL with EPAs. We first initialize the GNN model $f_{\text{pt}}(\cdot)$, encoder $f_{\text{enc}}(\cdot)$, and projection head $g(\cdot)$. It then pre-trains the GNN model on the labeled dataset \mathcal{T}_l for e_w epochs using cross-entropy loss. After that, a parametric GNN explainer $\Psi(\cdot)$ is trained on \mathcal{T}_l . To train the encoder, for each epoch, we sample minibatches from both labeled and unlabeled datasets. For each graph in the minibatch, we apply two randomly selected EPA techniques from the set EPA-Node Dropping, EPA-Edge Dropping, EPA-Attribute Masking, EPA-Subgraph, EPA-Mixup. These augmentations generate two views of each graph while preserving their critical structures. The algorithm then computes the self-supervised loss using either the contrastive loss or the SimSiam loss, depending on the chosen framework. Finally, it updates the encoder and projection head by minimizing this self-supervised loss.

Algorithm 6 EPA-GRL Algorithm

Input: Labeled dataset \mathcal{T}_l , unlabeled dataset \mathcal{T}_u , GNN pre-train epochs e_w , contrastive learning epochs e_s , temperature τ , batch size N

Output: Trained GNN encoder $f_{\text{enc}}(\cdot)$, trained explainer $\Psi(\cdot)$

```

1: Initialize GNN model  $f_{\text{pt}}(\cdot)$ , encoder  $f_{\text{enc}}(\cdot)$ , and projection head  $f_{\text{pro}}(\cdot)$ 
2: for epoch = 1 to  $e_w$  do
3:   for each  $G_i \in \mathcal{T}_l$  do
4:     Update  $f_{\text{pt}}$  via the Cross-Entropy Loss, Eq.(1)
5:   end for
6: end for
7: Train parametric GNN explainer  $\Psi(\cdot)$  using  $\mathcal{T}_l$  with Eq.(2)
8: for epoch = 1 to  $e_s$  do
9:   for sampled minibatch  $\{G_i\}_{i=1}^N$  from  $\mathcal{T}_l \cup \mathcal{T}_u$  do
10:    Sample  $t, t'$  from {EPA-Node Dropping, EPA-Edge Dropping, EPA-Attribute Masking, EPA-Subgraph, EPA-Mixup}
11:     $G_{i,1} = t(G_i, \Psi)$ 
12:     $G_{i,2} = t'(G_i, \Psi)$ 
13:   end for
14:   Compute self-supervised loss using Eq.(3) or Eq.(6)
15:   Update  $f_{\text{enc}}(\cdot)$  and  $f_{\text{pro}}(\cdot)$  by minimizing self-supervised loss
16: end for
17: return  $f_{\text{enc}}(\cdot), \Psi(\cdot)$ 

```

C Full Experimental Setups

C.1 Datasets

MUTAG [18]. MUTAG dataset contains 4,337 molecules. These molecules are split into two groups based on their mutagenic effects on Salmonella Typhimurium, a Gram-negative bacterium.

Benzene [1]. Benzene consists 12,000 molecular graphs. They are divided into two categories: one where the molecules contain benzene rings and another where the benzene ring is absent.

Alkane-Carbonyl [1]. The Alkane-Carbonyl has 4,326 molecular graphs. It is divided into two categories. The positive samples with ground-truth explanations include alkanes and carbonyl functional groups in the given molecules.

Fluoride-Carbonyl [1]. The Fluoride-Carbonyl dataset contains 8,671 molecular graphs. The ground-truth explanation depends on the specific combination of fluoride atoms and carbonyl functional groups found in each molecule.

D&D [9]. It contains 1,178 protein graphs, classified into two binary categories: enzymes and non-enzymes. Each node in the graph represents an amino acid. If the distance between two amino acids is within 6 Angstroms, the corresponding nodes will connect to each other by edges.

PROTEINS [4, 9]. The PROTEINS dataset consists of 1,113 protein graphs, following the same construction method as D&D. The statistics of all datasets are summarized in Table 5.

C.2 Baselines

GraphCL [43]. GraphCL is a framework for unsupervised graph representation learning. It applies four types of graph augmentation

Table 5: Statistics of datasets used for graph classification task.

Dataset	Domain	#Graphs	Avg.#nodes	Avg.#edges	#Explanations	#Feature	#Classes
MUTAG	Biochemical molecules	2,951	30.32	30.77	1,015	14	2
Benzene	Biochemical molecules	12,000	20.58	43.65	6,001	14	2
Alkane-Carbonyl	Biochemical molecules	4,326	21.13	44.95	375	14	2
Fluoride-Carbonyl	Biochemical molecules	8,671	21.36	45.37	1,527	14	2
D&D	Bioinformatics	1,178	284.32	715.66	0	89	2
PROTEINS	Bioinformatics	1,113	39.06	72.82	0	3	2

methods: node dropping, edge dropping, attribute masking, and sub-graph sampling. The code is available at <https://github.com/Shen-Lab/GraphCL>.

SimSiam [7]. SimSiam does not require negative samples, large batches, or momentum encoders to train GNNs. It relies on a stop-gradient operation to prevent collapsing solutions. The code is available at <https://github.com/leaderj1001/SimSiam>.

AD-GCL [28]. This framework optimizes adversarial graph augmentations to prevent GNNs from learning redundant information. It uses trainable edge-dropping strategy to enhance the robustness of GNNs. The code is available at <https://github.com/susheels/adgcl>.

JOAO [42]. JOAO uses min-max optimization to dynamically select data augmentation methods, allowing the augmentation strategy to adjust during training. The code is available at https://github.com/Shen-Lab/GraphCL_Automated.

AutoGCL [40]. It is an automatic graph contrastive learning framework that uses learnable generators with auto-augmentation to preserve key graph structures while introducing variance augmentation and jointly train the generator, encoder and classifier. The code is available at <https://github.com/Somedaywilldo/AutoGCL>.

SimGrace [34]. SimGrace does not require data augmentation. It uses the original graph as input and applies both the GNN and its perturbed version as two encoders to obtain two correlated views for contrastive learning. The code is available at <https://github.com/junxia97/SimGRACE>.

D Additional Experiments

Table 6: Comparison of different graph augmentation methods on two other datasets.

Augmentation Method		BA-2motifs	HIV
Node Dropping	Vanilla	0.739 \pm 0.126	0.634 \pm 0.032
	EPA	0.874 \pm 0.148	0.643 \pm 0.028
Edge Dropping	Vanilla	0.603 \pm 0.127	0.640 \pm 0.034
	EPA	0.701 \pm 0.197	0.636 \pm 0.032
Attribute Masking	Vanilla	-	0.621 \pm 0.017
	EPA	-	0.632 \pm 0.015
Subgraph	Vanilla	0.781 \pm 0.145	0.638 \pm 0.033
	EPA	0.786 \pm 0.180	0.640 \pm 0.018
Mixup	Vanilla	0.691 \pm 0.164	0.632 \pm 0.019
	EPA	0.694 \pm 0.143	0.642 \pm 0.016

D.1 Experiments on Synthetic and Large Scale Datasets

To further demonstrate the robustness of EPA on different types of data, we conduct experiments with the GraphCL framework on a synthetic dataset BA-2motifs[18] and a larger real-world dataset HIV[20]. The BA-2motifs dataset [18] contains 1,000 synthetic graphs generated from a standard Barabási-Albert (BA) model. The dataset is split into two groups: one set of graphs incorporates patterns resembling a house structure, while the other set integrates five-node cyclic motifs. The HIV dataset [20] consists of 41,127 molecular graphs, each representing a compound tested for its ability to inhibit HIV replication. The dataset is divided into two categories: one contains active molecules that can effectively inhibit HIV, and the other contains inactive molecules that lack inhibitory activity. The results are shown in Table 6. We find that our method achieves the best results across almost all data augmentation methods. Specifically, on the BA-2motifs dataset, our method improves by an average of 17.3% compared to Vanilla. Note that, since the node features in BA-2motifs have only one dimension, the feature masking augmentation method cannot be applied.

Table 7: Comparison of different graph augmentation methods with GIN as the backbone.

Augmentation Method		MUTAG	PROTEINS
Node Dropping	Vanilla	0.843 \pm 0.033	0.636 \pm 0.070
	EPA	0.846 \pm 0.035	0.646 \pm 0.074
Edge Dropping	Vanilla	0.836 \pm 0.023	0.637 \pm 0.049
	EPA	0.831 \pm 0.033	0.650 \pm 0.063
Attribute Masking	Vanilla	0.827 \pm 0.040	0.622 \pm 0.057
	EPA	0.838 \pm 0.027	0.656 \pm 0.075
Subgraph	Vanilla	0.830 \pm 0.029	0.633 \pm 0.045
	EPA	0.839 \pm 0.031	0.650 \pm 0.051
Mixup	Vanilla	0.842 \pm 0.038	0.625 \pm 0.087
	EPA	0.846 \pm 0.018	0.623 \pm 0.072

D.2 Experiments with Another Backbone

To evaluate the generalizability of our approach, we conduct additional experiments using a Graph Isomorphism Network (GIN) [39] as the backbone encoder. We focus on the MUTAG and PROTEINS datasets for this analysis. Table 7 presents the results of these experiments. We observe that EPA consistently outperforms the Vanilla augmentation methods in graph classification tasks on both datasets. This improvement suggests that the effectiveness of our

explanation-preserving augmentation method is not limited to a specific graph neural network architecture. Instead, it appears to enhance the performance of different types of graph encoders, further validating the robustness and versatility of our approach.

D.3 Additional Visualization

We present visual examples from all real datasets: MUTAG, Benzene, Alkane-Carbonyl, Fluoride-Carbonyl, D&D, and PROTEINS to demonstrate the semantic preservation ability of different augmentation techniques. The visualizations are shown in Figure 7. From the figure, we observe that the distribution difference between the original graph and the “Random-Aug” graph is large, while the difference between the original graph and the “EPA-Aug” graph is small. Although “Random-Aug” provides diverse augmentations, it may change key properties of the graph, affecting downstream tasks that rely on consistent graph semantics. This highlights the importance of semantic-preserving augmentations.

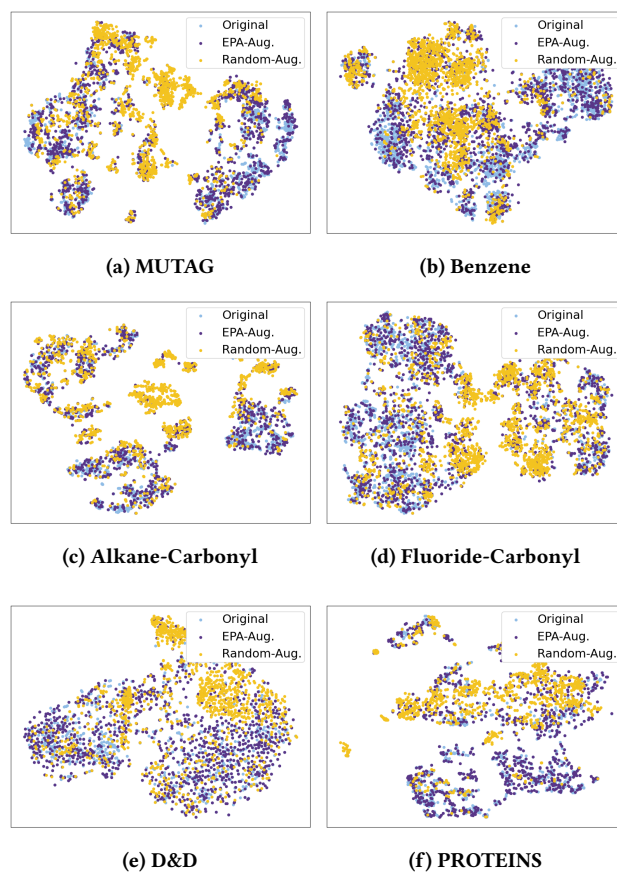


Figure 7: Visualizations of graph representations on all datasets.